UNIVERSITY OF MASSACHUSETTS/AMHERST
ENERGY ALTERNATIVES PROGRAM

Final Report

WIND TUNNEL TEST PROGRAM OF A 200-WATT, 12-VOLT WIND GENERATOR SYSTEM

by

F. S. Stoddard

M. Edds

U.Mass. Wind Furnace
Energy Alternatives Program
University of Massachusetts
Amherst, Massachusetts 01002

April 1976

TR/76/10

TABLE OF CONTENTS

LIST OF FIGURES

LIST OF TABLES

INTRODUCTION

In March, 1974, a small wind generator was purchased under the Mark Swann Account for the Energy Alternatives Program of the University of Massachusetts Engineering Department. The wind generator (Reference 1) was acquired as a demonstration, teaching, and research tool, and serves as a test stand in the University of Massachusetts Open Jet Wind Tunnel Facility (Reference 2). During the time period 15 March to 15 July, 1974, the wind generator system was fully tested and calibrated in the wind tunnel facility, and has been used since then as a valuable teaching and research aid in the Energy Alternatives Program.

An additional test hub was manufactured in April, 1974, and several model blades were run during a practical windpower course offered through the School of Continuing Education on the Amherst campus. These model blades were constructed by the class members primarily as a teaching technique, and were never intended to be rigorous wind tunnel models. However, the results of that program did amplify observations concerning small scale wind generators (see Part 8: Conclusions and Observations). During the Fall and Spring semesters, 1974-1975, two graduate engineering courses were offered in the Civil, and Mechanical and Aerospace Engineering Departments, on Windpower Systems Engineering, as part of the Energy Alternatives Program. The wind tunnel test experience with the model rotors served as valuable background and demonstration for the courses. Since then, further blade performance research has been accomplished in the wind tunnel facility under National Science Foundation sponsorship (NSF Grant AER-00603).

GET MAXIMUM POWER FROM THE FREE WIND WITH A HEAVY DUTY 12 VOLT

12 VOLT WIND ELECTRIC BATTERY CHARGER

MODEL NO. 1222H WIND ELECTRIC BATTERY CHARGER

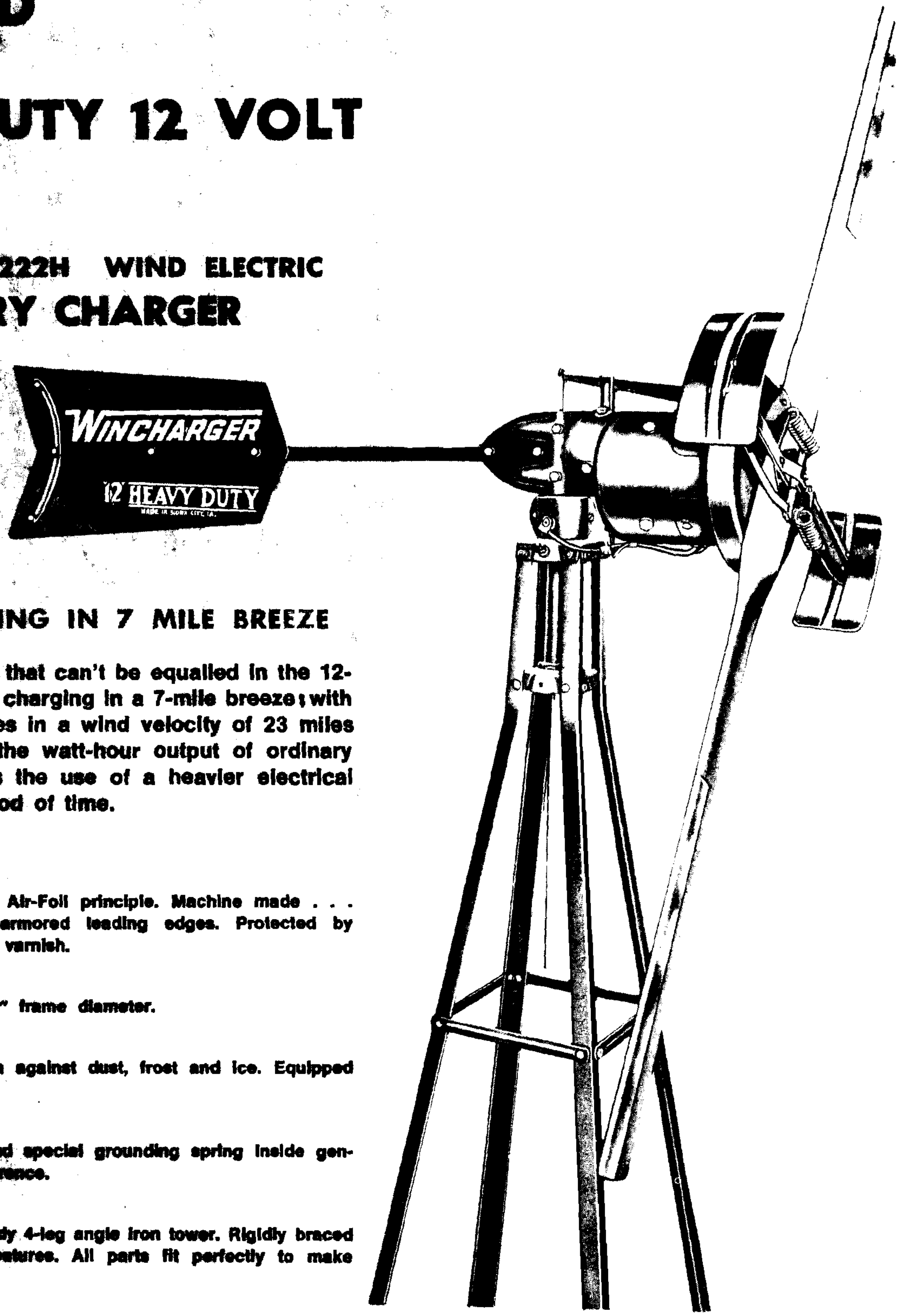

STARTS CHARGING IN 7 MILE BREEZE

All-around performance that can't be equalled in the 12-volt lighting field. Starts charging in a 7-mile breeze; with an output of 15 amperes in a wind velocity of 23 miles per hour. Has double the watt-hour output of ordinary radio chargers. Permits the use of a heavier electrical load over a longer period of time.

Built on the famous Albers Air-Foil principle. Machine made . . . perfectly balanced. Copper-armored leading edges. Protected by three coats of weather-proof varnish.

Bearings grease sealed. 7½" frame diameter.

Provides complete protection against dust, frost and ice. Equipped with double carbon brushes.

Condensers on generator and special grounding spring inside generator eliminate radio interference.

Model 1222H mounts on sturdy 4-leg angle iron tower. Rigidly braced . . . newest construction features. All parts fit perfectly to make erection simple.

WINCO
Division of DYNA TECHNOLOGY, INC.
SIOUX CITY, IOWA 51102

FIGURE 1

CHARGING CURRENT VS. RPM

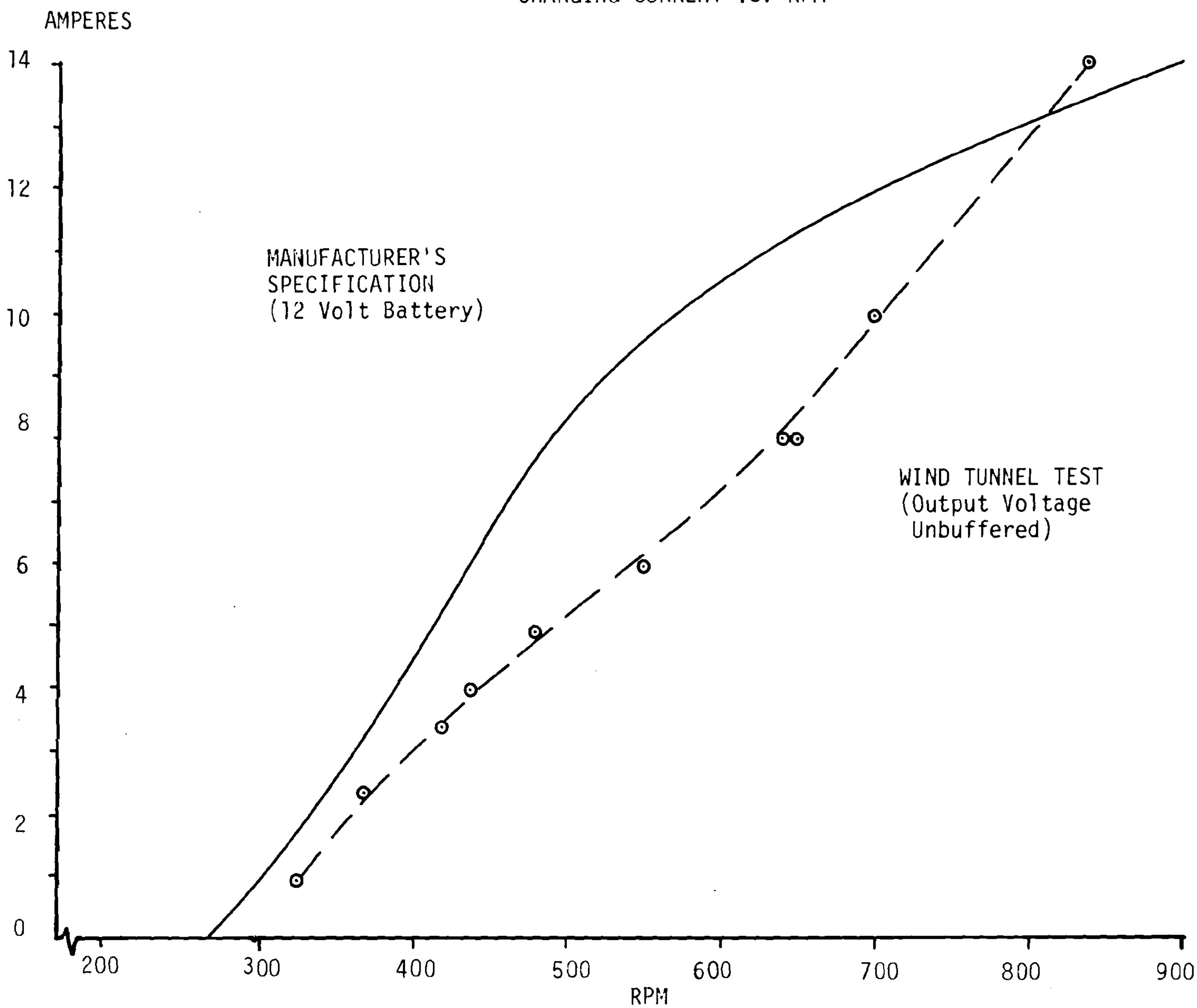

FIGURE 1

WIND GENERATOR: GENERAL DESCRIPTION

A. Background

The Wincharger Model No. 1222H Wind Electric Battery Charger is a small, 12 volt battery charging system produced by Dyna Technology, Inc., Sioux City, Iowa (Reference 1). It was, in 1974, the only U.S.-produced, commercially-available wind generator and sold for approximately $450.00 on a 10' stub tower. This particular system was designed and marketed in essentially identical form some 40 years ago, first by Wincharger, Inc., and then Zenith, up to 1968, when the design and tooling were acquired by Dyna Technology. The only differences in the current machine, are the larger generator casting (which is now wider at 7" diameter), and the blade, which is now redwood, instead of Sitka spruce. The wind generator was designed for charging a 6-cell, 12 volt house lighting battery for rural use. These units are now in production, and many thousands are being used successfully throughout this country. The output is so small, though (less than 250 kWh annually in most areas) that it represents only a tiny application of solar energy, or only serves hobby interests. It does, however, provide an excellent small scale test stand for wind generator research.

B. System Description

The manufacturer's specifications for the Model 1222 are given in Table 1, along with other machines since discontinued by Wincharger, Inc. and Dyna Technology. It is interesting to note that the only current survivor is the smallest, simplest system, and is the only machine with a direct drive (no gearing). The 12-volt, DC shunt

TABLE 1: ENGINEERING DATA SPECIFICATIONS
WINCHARGER UNITS
July 1, 1953

MODEL NUMBER	1112	3240	3242	1222	623	611
Propeller Type	4 Blade	4 Blade	2 Blade	2 Blade	2 Blade	2
Size	14 Feet	14 Feet	10 Feet	6 Feet	6 Feet	
Material	Aluminum	Aluminum	Wood	Wood	Wood	
Gear Ratio	6.14	6.14	4.	Direct	Direct	
Generator	8" Dia. 2 Pole	8" Dia. 2 Pole	7 1/2" Dia. 4 Pole	7 1/2" Dia. 4 Pole	4 1/2" Dia. 2 Pole	
Capacity (Watts)	1500	1350	1000	200	90	100
Gen. Speed Range (RPM)	*800/1350	840/1350	850/1375	260/700	300/1150	
Governor Type	Variable-Pitch	Variable-Pitch	48" Air-Brake	22" Air-Brake	22" Air-Brake	
Prop. Speed Range (RPM)	*131/220	137/330	212/345	260/700	300/1150	
Wind Speed Range (MPH)	*7/20	7/19	9/23	7/23	9/25	
Voltage Regulator	Yes	Yes	No	No	No	
Approx. Max. Amps	11	30	25	14	13	
Approx. Max. Volts	140	40	40	15	7.5	
No. Battery Cells	56	16	16	6	3	
Volts per cell (When fully charged**)	2.5	2.5	2.5	2.5	2.5	
Size Battery Recommended ("WINCHARGER" Trademark)	13S	19H	19H	19H	13H	
Avg. Usable KWH per month						
10 MPH Annual Avg.	172	160	60	20	10	
12 MPH Annual Avg.	224	200	90	26	13	
14 MPH Annual Avg.	278	230	122	30	15	

EXPLANATIONS: *Wind and Propeller and Generator speed ranges as given indicate first the speed that is required to begin charging the battery and then the speed required for the governor to begin operation.

For Example: On Model 1112, the propeller begins charging the battery at 131 RPM which corresponds to a generator speed of 800 and a wind speed of 7 MPH. Governing speed is reached at 220 RPM, which corresponds to a generator speed of 1350 and a wind speed of 20 MPH.

** For lead acid batteries only.

generator is rated at 200 watts at 700 RPM, and begins charging at 260 RPM. The corresponding wind speed range is 7 to 23 MPH (see Figure 1).

1. Propeller

The 6-foot (3-foot radius) redwood propeller has a constant chord of 3.5", and zero twist. The airfoil section is a conventional, lightly cambered airfoil of approx. 15% thickness, with a blunt trailing edge. Surface roughness is high, and is severely aggravated by a leading edge copper erosion strip stapled on the outer 50% of the span. The tips are lightly rounded but not elliptical. The bending and torsional stiffnesses are very high, but were not measured in this test.

2. Control System

The propeller control system is an "Albers governor air brake": a spring-loaded centrifugal flyweight, designed to increase rotational drag at high RPM by deploying curved air brakes from an equilibrium position at 0.3 radius. A manual hand brake is included; it is a cast brake shoe activated against a 9" drum through a vertical cable down the tower axis. Yaw control moments are provided by a vertical stabilizer.

3. Structure

The structure of the aloft system is the cast generator housing, which serves as the load path for all hub loads and generator rotor loads. The housing is bolted to a rear flange assembly (generator mounting bracket) which is mated to the vertical tower support bearings, through which thrust, weight, drag and moments are transmitted to the tower structure. The center of gravity of the yawing assembly is located at the tower axis by correct weighting of the tail boom and vertical stabilizer.

4. Generator

The generator is a 4-pole, 12 volt direct current shunt generator, with two armature brushes and a dual slip ring assembly for transmission down the tower. It is a rewound automobile generator with two main bearings. The generator has been changed little in the 40 years the unit has been marketed (Reference 4).

5. Loading Arrangement

A control panel consisting of a diode and heat sink in combination with an ammeter, is included for battery charging application. The normal load consists of a 6-cell, 12 volt house lighting battery. The test program did not use the control panel.

6. General Construction

The system is simple and direct, designed with long reliability and low maintenance in mind. The generator and permanently-sealed bearings are isolated from the weather by access panels and gaskets. The tower slip ring assembly is completely sealed, and the entire unit is corrosion-protected.

GENERATOR TEST

A. Measurement of Field and Armature Resistances

The simple DC shunt generator circuit diagram is shown in Figure 2:

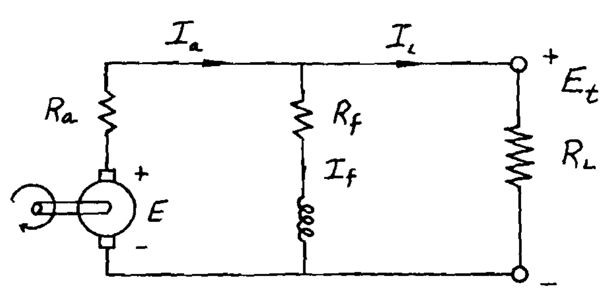

FIGURE 2

FIELD VOLTAGE VS. FIELD CURRENT

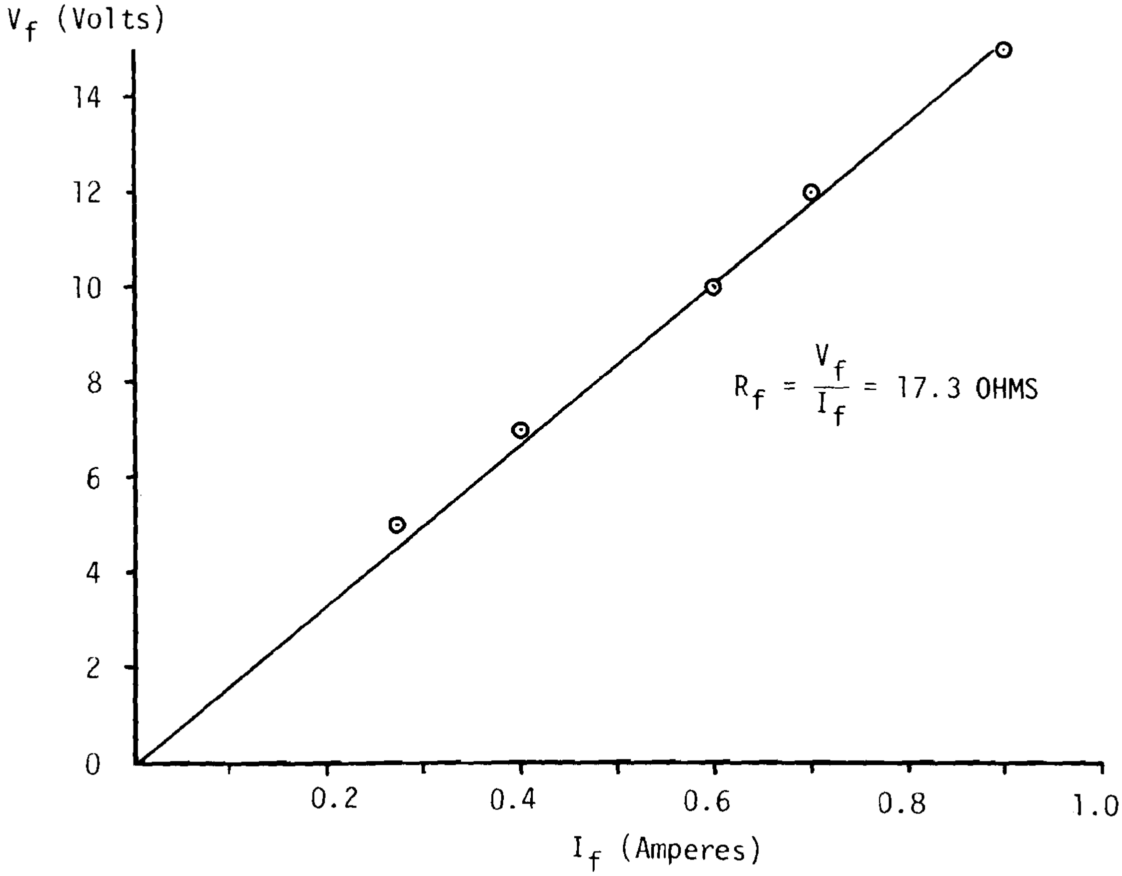

FIGURE 3

ARMATURE VOLTAGE VS. ARMATURE CURRENT

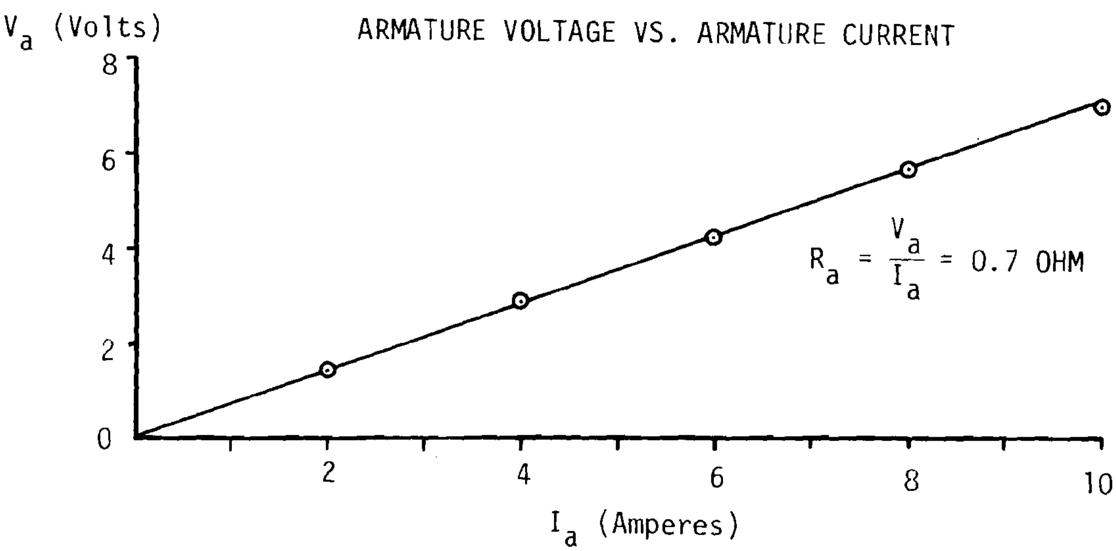

FIGURE 4

where: E = armature (generated) voltage

R_a = armature resistance

R_f = field resistance

R_L = load (terminal) resistance

E_t = load (terminal) voltage

I_L = load (terminal) current

E_f = field current

I_a = armature current

Unknowns R_a and R_f were measured by isolating the armature and the field circuits by removing the brushes. Then an external (known) voltage was applied to each, and the resulting current was measured. From the results, see Figures 3 and 4, the resistances were measured as the respective slopes.

B. Measurement of Real Losses

In order to measure the real losses of the DC generator, it was necessary to isolate the field and run the machine as a separately-excited DC motor as shown in Figure 5.

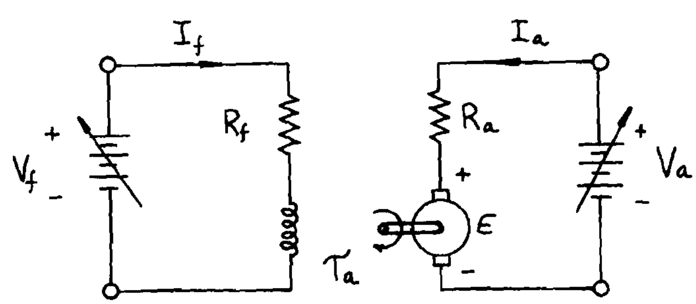

FIGURE 5

where: V_f = applied field voltage

V_a = applied armature voltage

τ_a = rotor torque = 0

For the armature circuit, including a 2 volt armature loss (by convention):

$$E = V_a - I_a R_a - 2 \text{ volts} \tag{1}$$

The power in the armature can be written:

$$P_a = V_a I_a = EI_a + I_a^2 R_a + 2I_a \tag{2}$$

The test then proceeded to measure the losses in the armature by the following method:

(a) Field excitation, V_f, was set at a constant level; knowing $R_f = 17.3\Omega$, this made I_f a constant for the test.

(b) The applied armature voltage, V_a, was varied and the rotor was allowed to turn with no external load (i.e. $\tau_a = 0$); this means the power loss in the armature was attributable to real losses.

(c) The rotor RPM was recorded as V_a was varied, and a resulting table included RPM, V_a, I_a, and V_f.

The real losses in the armature were due to friction, windage (air gap) and magnetization (core loss). Since the torque was zero, the EI_a in (2) represented the power that is dissipated by losses. Thus:

$$P_{losses} = EI_a = V_a I_a - 2I_a - I_a^2 R_a \tag{3}$$

Equation (3) was used to calculate the losses; they are plotted in Figure 6.

The overall power equation for the DC shunt generator, Figure 2, can then be written:

$$P_{\substack{\text{mechanical}\\ \text{input}}} = P_{\substack{\text{terminal}\\ \text{output}}} + 2I_a + I_a^2 R_a + I_f^2 R_f + P_{losses} \tag{4}$$

POWER LOSSES DUE TO FRICTION, WINDAGE, AND CORE

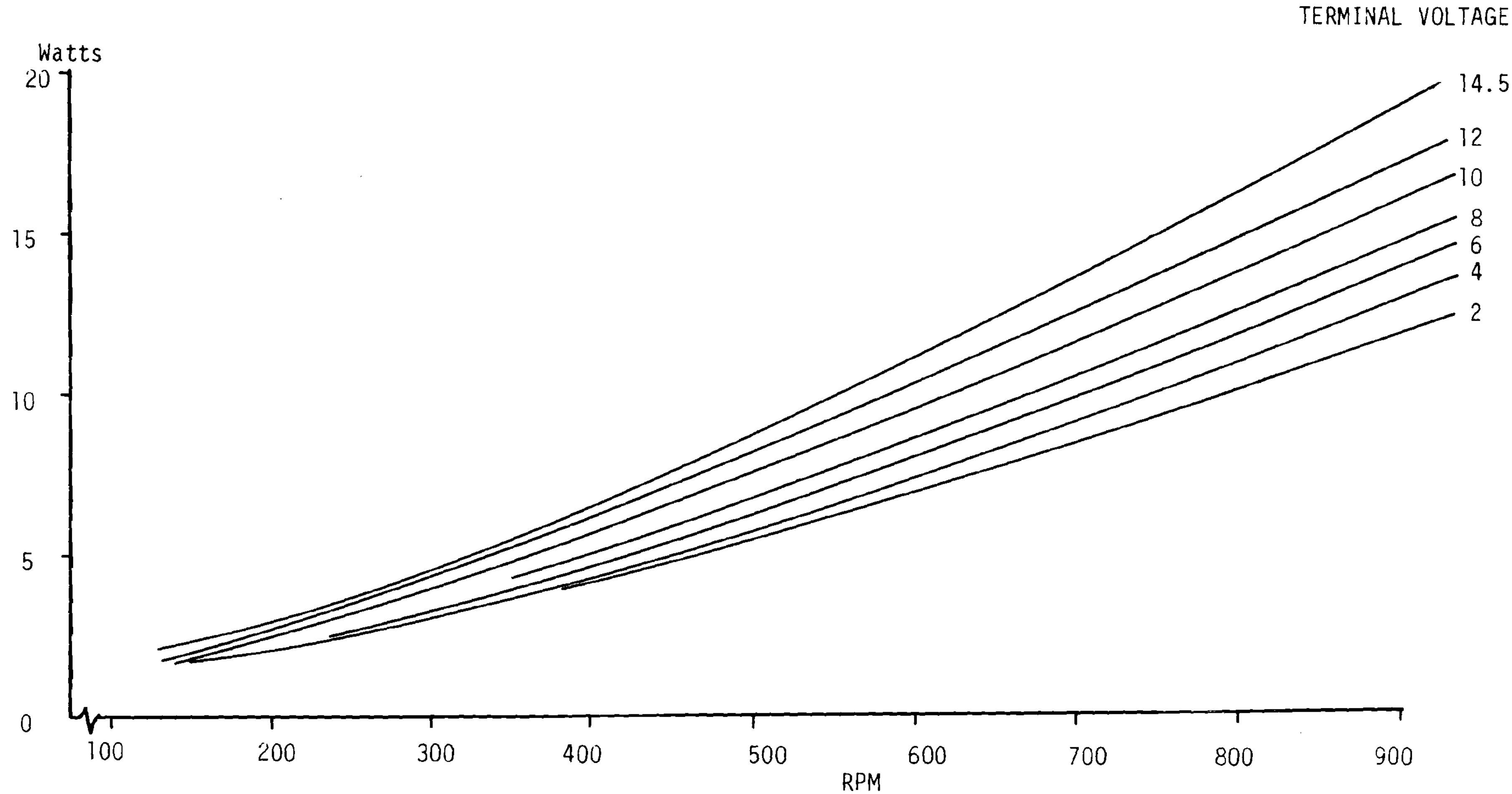

FIGURE 6

This relationship was used to evaluate the generator performance used in this test program. Section 7 describes the analysis which separated the propeller input power from the system power.

WIND TUNNEL DESCRIPTION

The wind tunnel used in this test was an open jet wind tunnel constructed on the Amherst campus under Project Themis Contract ONR-N00014-68-A-0146-12 (Reference 2). The test setup can be seen in Figures 7 and 8. The open jet face was 4 feet square, and exhausted into a large bay and through the facing outer wall. The model dimension was an actuator disc six feet in diameter, clearly larger than the tunnel jet. However, despite the uncertainty of absolute measurements, it is felt that correlative and comparative data were accurate. Also, the facility was open jet, thus elminating the chronic wind tunnel testing problem of restricted wake expansion in closed test sections.

The testing arrangement is shown in Figure 9. The rotor was located far enough downstream from the jet face so that substantial turbulent mixing could occur. A turbulence generating screen was also fitted to the exit face. No wake velocity measurements were taken; the wake geometry upstream and downstream of the rotor was not measured.

Tunnel jet speed was measured with a pitot-static tube located at the tunnel face, the data reduction following established practice (Reference 5).

The governing calibration equation is:

$$w = 780\sqrt{h\gamma} \tag{5}$$

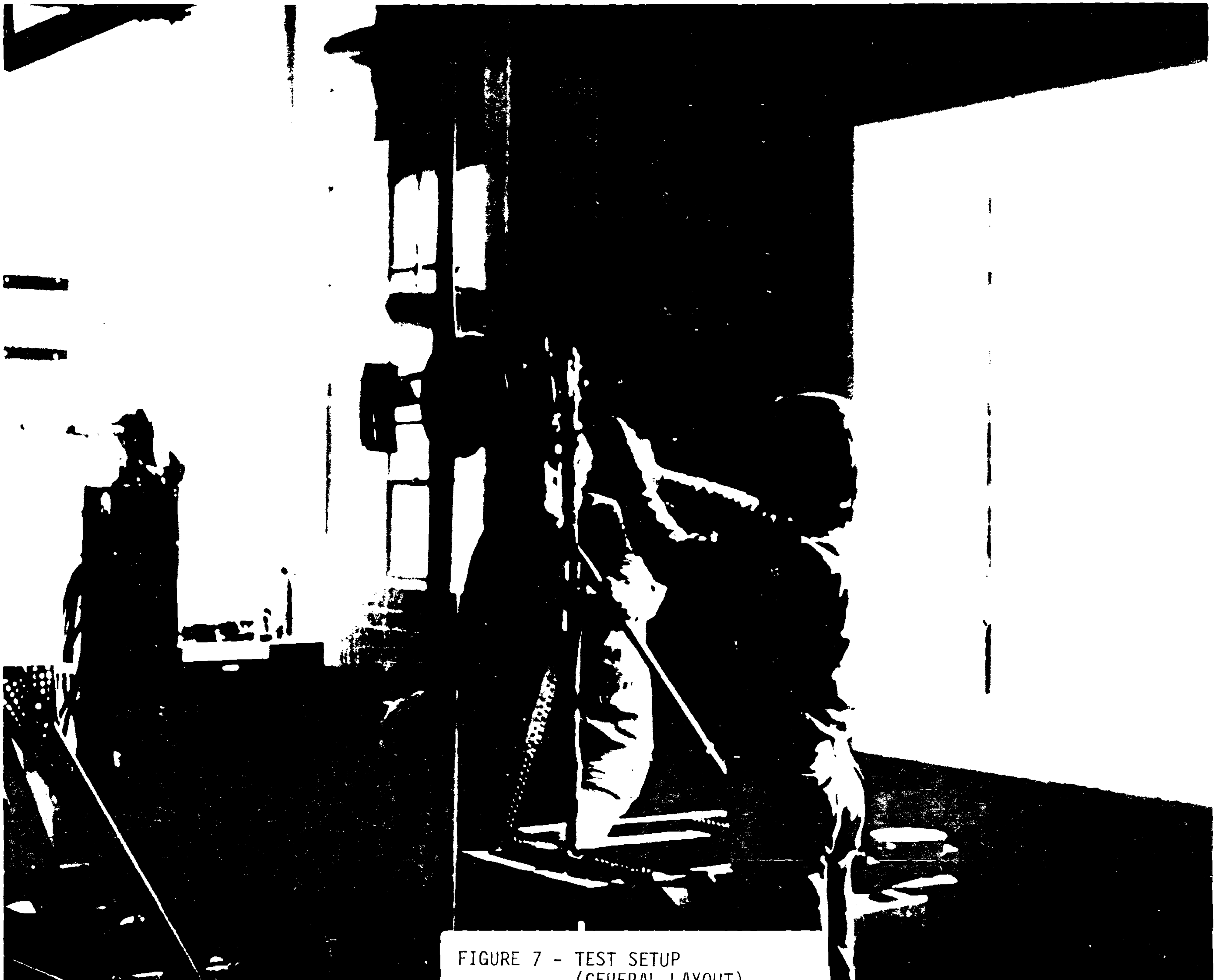

FIGURE 7 - TEST SETUP
(GENERAL LAYOUT)

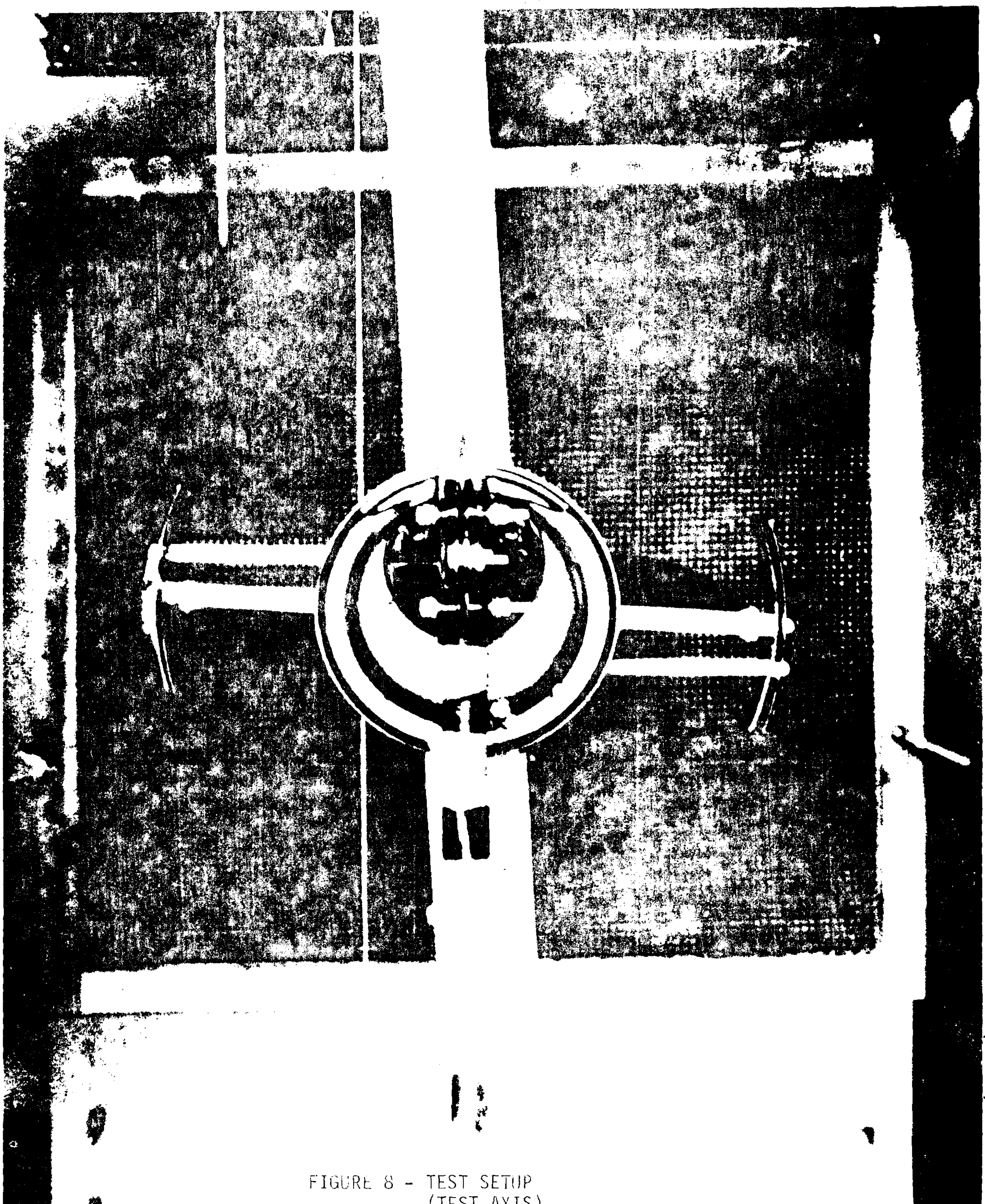

FIGURE 8 - TEST SETUP
(TEST AXIS)

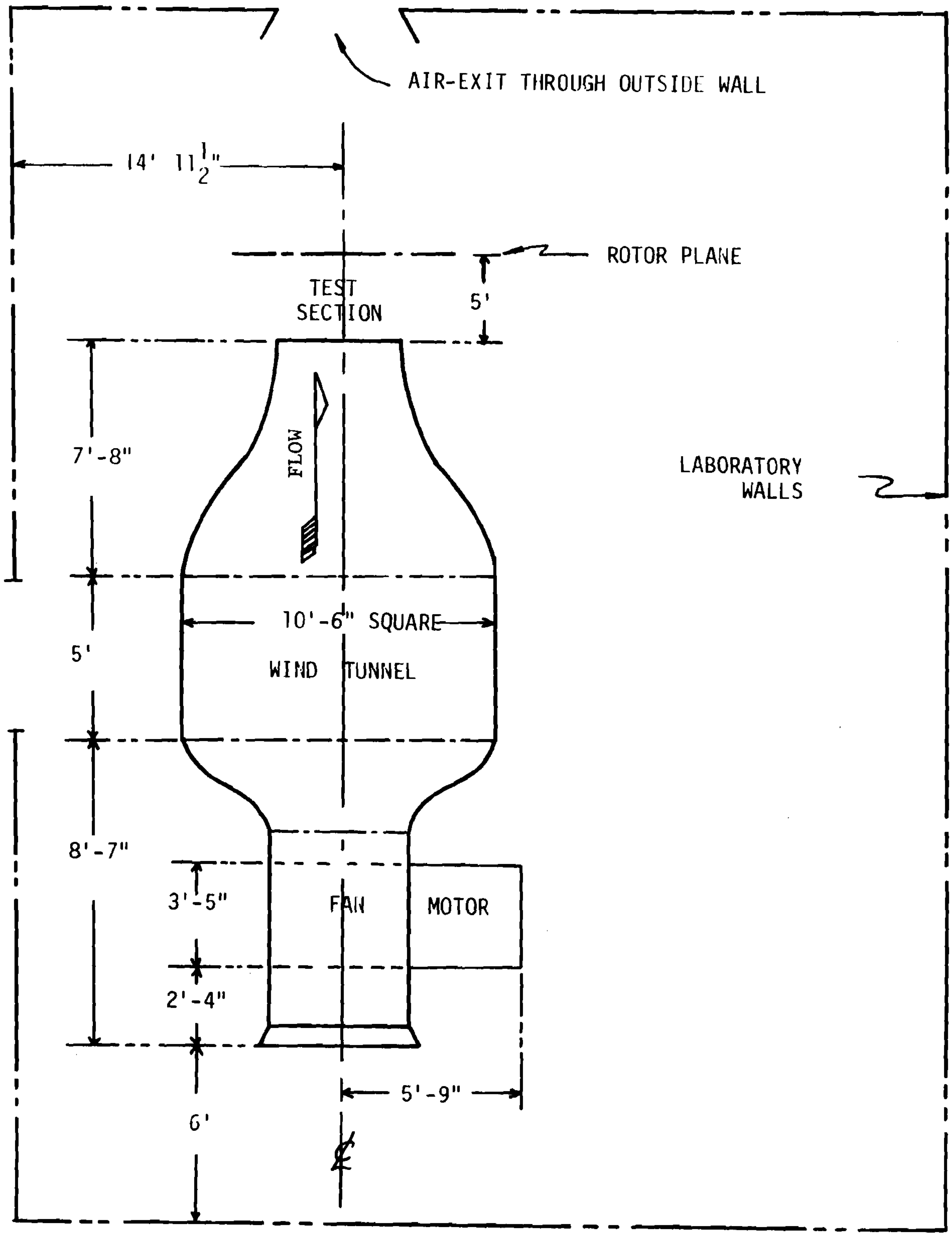

FIGURE 9 - TEST ARRANGEMENT

where: w = free stream speed (inches/sec.)

h = differential height of fluid in u-tube (inches)

γ = specific gravity of fluid

This gives the following result:

$$w(\text{ft/sec}) = 94.696\,[h]^{1/2} \qquad (6)$$

with γ = .834 (petroleum oil)

h = differential height in cm.

No corrections due to atmospheric pressure changes were made; and no wake effect corrections were made.

SYSTEM TEST PROCEDURE

A. Test Setup

The rotor system was securely fastened to a vertical mast, which was clamped to I-beam mountings on the floor (see Figure 7). The propeller rotational axis was rigidly aligned along the tunnel jet centerline using measuring tapes and plumb lines (see Figure 8).

The blades and air brake drum were assembled according to the manufacturer's booklet, and the blades were statically balanced and tracked. No balance weights were needed in addition to those already in place by the manufacturer. The dynamic tracking of the blades was also checked, and was satisfactory ($\pm$ 1 blade tip thickness).

B. Data Taking

The test system is diagrammed in Fig. 2. The variable resistance load consisted of a series of power resistors, or load racks, whose combined resistance could be changed from 0.5 to 25 ohms. No modifications were made to the generator circuit. The power leads to the data control area were 12 feet long, and were standard #8 copper wire.

The rotational speed (RPM) of the rotor was measured with a Honeywell Strobonar tachometer, and the load voltage and current were read from conventional voltmeters and ammeters. All instruments were re-zeroed and/or calibrated daily, and were re-checked prior to each new test run; no unusual calibration problems were noted with the simple instrumentation used.

C. Data Runs

The data survey schedule is shown in Table 2. Raw data are given in Appendix 1. The data were collected over the three day period: 29-31 March 1974.

TEST RESULTS: COMPLETE WIND GENERATOR SYSTEM

This section deals with the performance of the complete rotor/generator/transmission/load system as described. It is felt that these results are useful for comparative purposes with other small wind generators, even though it is understood that the mean jet velocity is probably conservative due to the small jet size (Section 5). Also, the parametric performance of the system was accurately measured.

A. Data Reduction

The experimental data were:

h = u-tube manometer fluid differential height (inches)

RPM = rotational speed of propeller

E_t = load terminal voltage

I = load terminal current

The jet velocity was found using the method described in Section 5. The power dissipated in the resistance load is simply the product of E_t and I; and the load resistance is simply E_t/I. Torque (net) is

TABLE 2: WINCHARGER TEST
DATA RUN SCHEDULE (29-31 March 1974)

Run	V_o	R_L	Comments
1	varied	0	No load (shorted) run at various V_o.
2	9.1 MPH	varied	Power Survey Runs
3	11.4	varied	Power Survey Runs
4	13.4	varied	Power Survey Runs
5	17.5	varied	Power Survey Runs
6	19.5	varied	Power Survey Runs
7	22.0	varied	Power Survey Runs
8	13.4	varied	Repeated power surveys
9	22.0	varied	Repeated power surveys
10	24.0	varied	Repeated power surveys
11	15.0	varied	Repeated power surveys
12	30.0	varied	Repeated power surveys
13	varied	3Ω	Velocity Survey Runs
14	varied	4	Velocity Survey Runs
15	varied	5	Velocity Survey Runs
16	varied	6	Velocity Survey Runs
17	varied	0.5	Velocity Survey Runs
18	varied	2Ω	Velocity Survey Runs
19	7 MPH	varied	Power Survey Run

power divided by rotational speed. These data can be seen in Appendix 1.

B. Power and Torque vs. RPM

The power and torque characteristics are shown in Figures 10 and 11 for various tunnel speeds. The abscissa interceptions (circled) represent a separate test run with the generator leads shorted (i.e. zero resistance) as a no load check. The error was due to the difficulty in reestablishing an exact wind tunnel jet velocity (velocity survey run).

Power survey runs were taken by establishing an equilibrium wind tunnel speed, and then varying load resistance, allowing the voltage and RPM transients to damp out before a data point was established. Usually the lowest resistance was used to start a run; this gave the data point with the lowest terminal voltage and the highest propeller RPM. Then the load resistance was varied in small increments, and the subsequent data points recorded. The terminal power is seen to increase, and the propeller RPM decrease until a maximum power is reached. Further load increases cause the terminal current to fall off drastically, while the terminal voltage continues to climb (see next paragraph). Power falls off drastically until an equilibrium point is reached, e.g. open circuit (infinite resistance).

C. Terminal Voltage and Current

Figure 12 shows a typical data run (V_0 = 13.4 MPH), showing the variation in RPM, E_t, and I with load resistance. As R_L is increased from zero (short circuit), terminal voltage and current climb rapidly, and RPM falls. At a certain R_L, current begins to fall off; this critical resistance was approximately 2 ohms in all cases. As R_L is increased

SYSTEM TERMINAL POWER VS. RPM

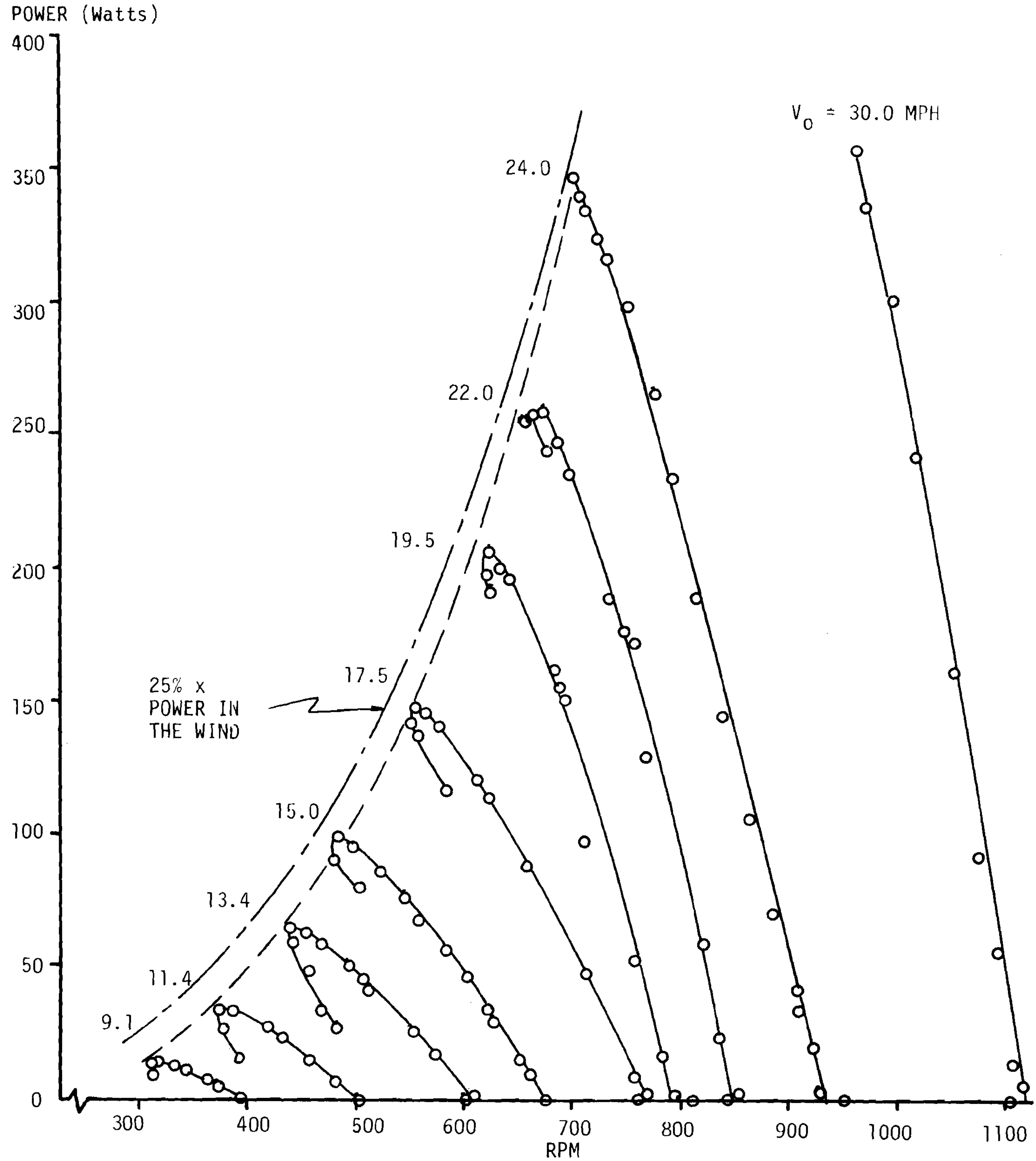

FIGURE 10

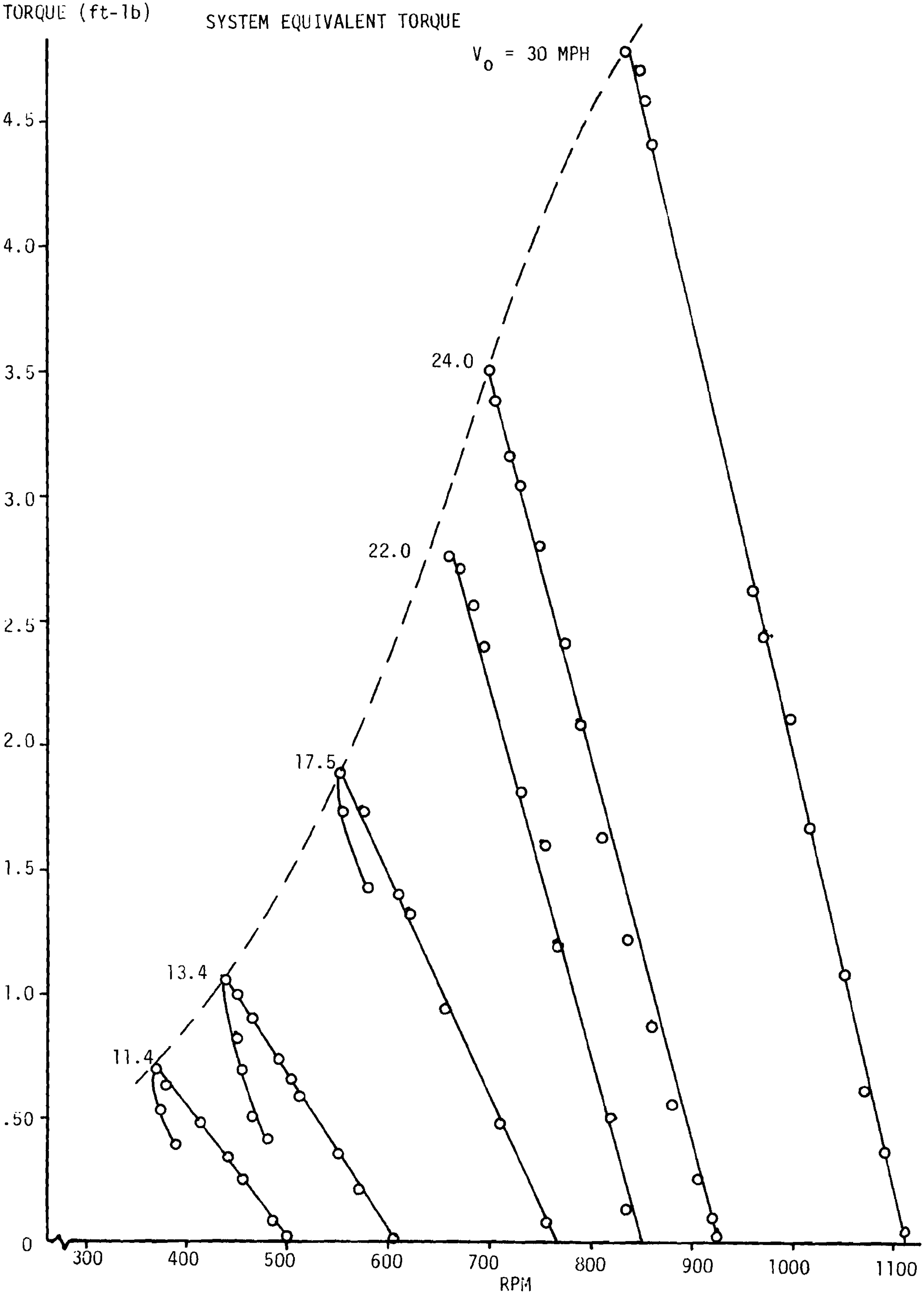
TORQUE (ft-lb)
SYSTEM EQUIVALENT TORQUE
V_o = 30 MPH
24.0
22.0
17.5
13.4
11.4
4.5
4.0
3.5
3.0
2.5
2.0
1.5
1.0
.50
0
300
400
500
600
700
800
900
1000
1100
RPM

FIGURE 11

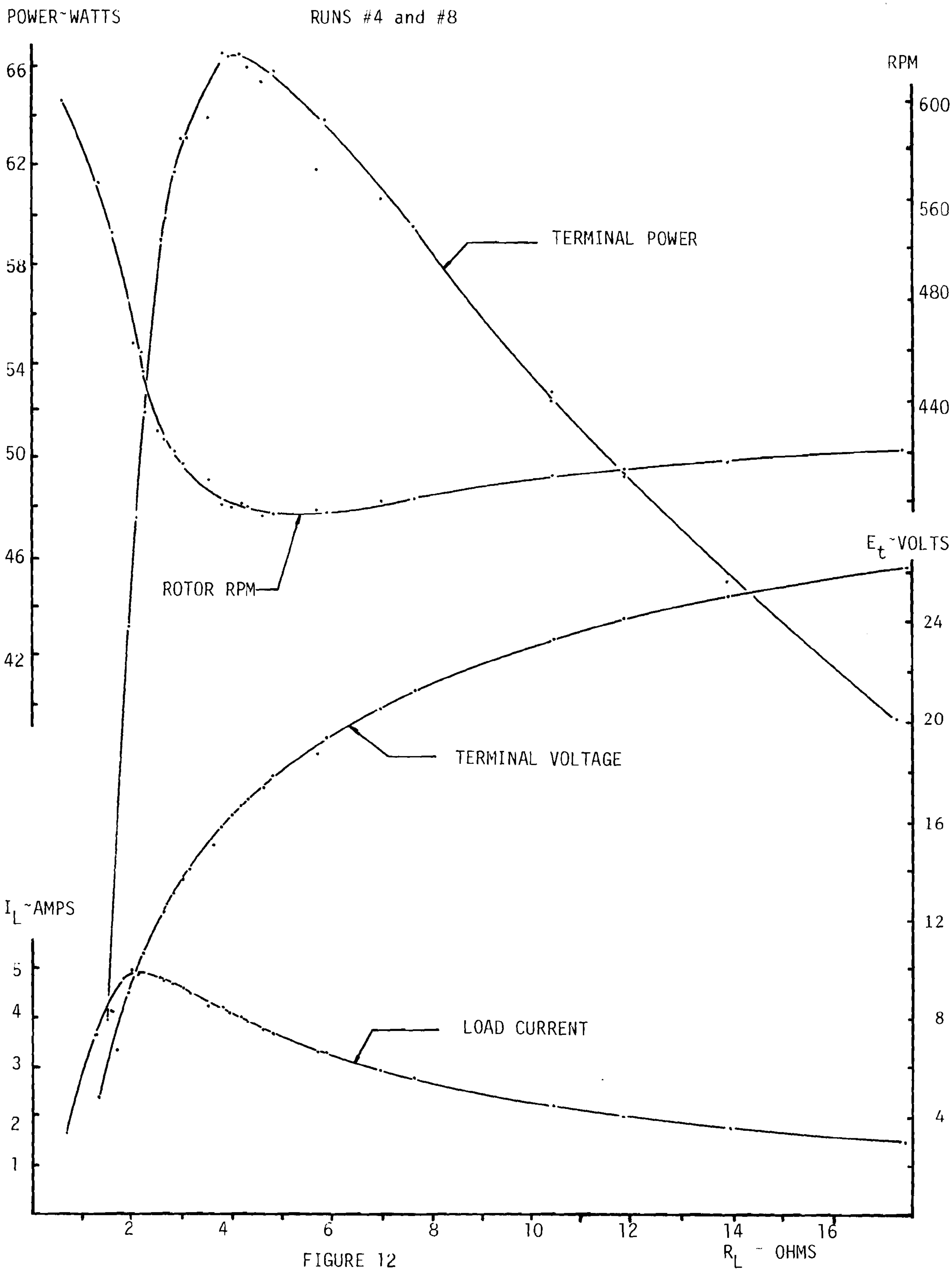

POWER~WATTS
RUNS #4 and #8
RPM
66
62
58
54
50
46
42
600
560
480
440
TERMINAL POWER
ROTOR RPM
E_t~VOLTS
24
20
16
12
8
4
TERMINAL VOLTAGE
I_L~AMPS
5
4
3
2
1
LOAD CURRENT
2
4
6
8
10
12
14
16
R_L ~ OHMS

FIGURE 12

further, a power peak coincides with the lowest propeller RPM. Power and current fall rapidly as terminal voltage continues to rise to the infinite resistance value (open circuit); RPM is practically constant, falling off somewhat. Figure 12 includes data taken in reverse order; that is, a high load resistance was used to start, and the power peak was approached from the right-hand side. The different sets of data are clearly compatible.

D. Power vs. Load Resistance

The system performance is probably best measured by the output power vs. load resistance for various wind speeds, Figure 13. It can be easily seen that the power peaks all occur at about 4 ohms, and that the characteristics are very sensitive to load changes at less than 3 ohms. This suggests an optimum load for the equilibrium system tested. Generator efficiency also peaks at 3-4 ohms load (Section 8, Figure 18).

TEST RESULTS (ROTOR)

Wind generator propeller performance is generally given as a power coefficient vs. tip speed ratio, or non-dimensional power vs. rotational speed for a constant wind speed:

$$C_p = \text{power coefficient} = \frac{P}{\frac{1}{2}\rho A V_o^3} \qquad (7)$$

$$\mu = \text{tip speed ratio} = \frac{\Omega R}{V_o} \qquad (8)$$

It is unnecessary to find C_p vs. μ for more than one wind speed; the (ungoverned) characteristic will be the same, disregarding the (unknown) effect of Reynold's number ($Re = \frac{\rho V c}{\mu}$) on drag and differences in the wake geometry.

OUTPUT POWER VS. LOAD RESISTANCE

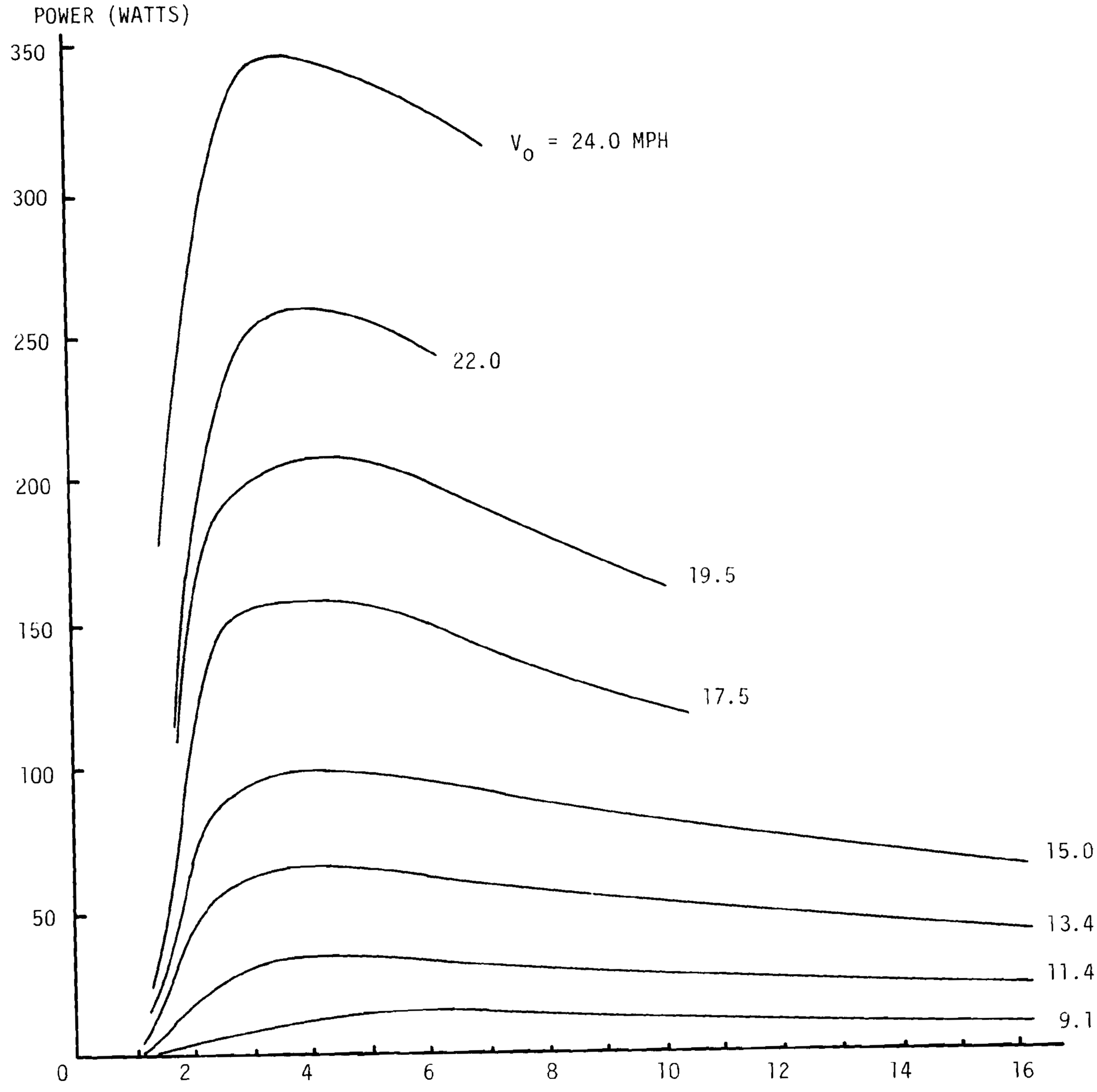

FIGURE 13

A. Data Reduction

The governing equation for the power in a DC shunt generator (Figure 2) is:

$$P_{\substack{\text{mechanical}\\ \text{input}}} = P_{\text{output}} + P_{\text{circuit}} + P_{\substack{\text{real}\\ \text{losses}}} \tag{9}$$

The mechanical input is the (direct) power given by the propeller shaft and the output is the power dissipated in the heating load. The real losses are due to friction, windage and magnetization, and were found (Section 4). The equation thus becomes:

$$P_{\text{shaft}} = E_t I + 2I_a + I_a^2 R_a + I_f^2 R_f + P_{\text{losses}} \tag{10}$$

and:

$$I_f = \frac{E_t}{R_f}; \qquad I_a = I + I_f \tag{11}$$

This gives:

$$P_{\text{shaft}} = I[2 + IR_a + E_t\ (1 + 2\ \frac{R_a}{R_f})]$$
$$+ \frac{E_t}{R_f}\ [2 + E_t\ (1 + \frac{R_a}{R_f})] + P_{\text{losses}} \tag{12}$$

With $R_a = 0.7$, $R_f = 17.3$:

$$P_{\text{shaft}} = 2I + 0.7I^2 + 1.081\ E_t I + 0.116E_t + .06E_t^2 + P_{\text{losses}} \tag{13}$$

Data reduction constants were:

$$C_p = .002891 \times [P(\text{watts})] \tag{14}$$

$$\mu = .01599 \times [\text{RPM}] \tag{15}$$

$$C_Q = \text{torque coefficient} = C_p/\mu \tag{16}$$

Tables 3 and 4 give the reduced data for Runs #4 and #8 (V_o = 13.4 MPH).

TABLE 3: RUN #4
REDUCED DATA
V_o = 13.4 MPH

RPM	I	E_t	$P_{terminal}$	P_{total}	$\mu = \frac{\Omega R}{V_o}$	C_p	C_Q
478	.95	28.2	27.8	94.76	7.64	.274	.0359
465	1.25	27.2	34.0	99.19	7.43	.287	0.0386
460	1.5	26.2	39.3	102.39	7.35	.296	.0403
456	1.8	25.1	45.2	106.02	7.29	.307	.0421
454	2.05	24.2	49.6	108.8	7.26	.315	.0434
450	2.25	23.4	52.7	110.4	7.19	.319	.0444
450	2.25	23.3	52.4	110.9	7.19	.321	.0446
441	2.8	21.2	59.4	113.8	7.05	.329	.0467
440	2.95	20.5	60.5	113.8	7.03	.329	.0468
436	3.3	19.3	63.7	116.1	6.97	.336	.0482
435	3.7	17.8	65.9	117.4	6.95	.340	.0489
434	3.75	17.4	65.3	115.9	6.94	.335	.0483
438	3.9	16.9	65.9	116.6	7.00	.337	.0481
439	4.0	16.6	66.4	117.2	7.02	.339	.0483
438	4.1	16.2	66.4	117.1	7.00	.339	.0484
439	4.2	15.8	66.4	116.9	7.02	.338	.0481
449	4.25	15.0	63.8	112.9	7.18	.326	.0454
455	4.5	14.0	63.0	112.2	7.27	.324	.0446
455	4.6	13.7	63.0	112.2	7.27	.324	.0446
460	4.7	13.1	61.6	110.4	7.35	.319	.0434
465	4.75	12.6	59.9	108.1	7.43	.312	.0420
468	4.8	12.3	59.0	107.2	7.48	.310	.0414
492	4.9	10.6	51.9	98.0	7.87	.283	.0460
503	4.85	9.8	47.5	92.3	8.04	.267	.0332
512	4.8	9.0	43.2	86.0	8.19	.249	.0304
550	4.1	6.7	27.5	60.4	8.79	.175	.0199
570	3.6	4.8	17.3	44.1	9.11	.127	.0139
604	1.55	1.1	1.7	13.0	9.66	.038	.0039

TABLE 4: RUN #8
REDUCED DATA
V_o = 13.4 MPH

RPM	I	E_t	$P_{terminal}$	P_{total}	$\mu = \frac{\Omega R}{V_o}$	C_p	C_Q
604	1.5	1.21	1.82	12.9	9.66	.037	.00383
602	1.53	1.39	2.1	13.6	9.62	.039	.0041
602	1.8	1.9	3.4	16.8	9.62	.049	.0051
600	1.8	1.92	3.5	16.9	9.49	.049	.0051
594	1.85	2.0	3.7	17.4	9.50	.050	.0053
598	2.05	2.42	5.0	19.9	9.56	.058	.0061
586	2.35	3.15	7.4	24.5	9.37	.071	.0076
580	3.0	4.55	13.7	35.9	9.27	.104	.0112
571	3.3	5.3	17.5	42.5	9.13	.123	.0135
496	5.1	9.6	49.0	94.8	7.93	.274	.0346
468	4.9	11.9	58.3	107.1	7.48	.310	.0414
463	4.95	12.4	61.4	111.4	7.40	.322	.0435
448	4.7	14.1	66.3	117.6	7.16	.340	.0475
438	4.4	15.4	67.8	118.9	7.00	.344	.0491
422	3.35	19.5	65.3	118.5	6.75	.342	.0507
434	2.4	22.8	54.7	111.1	6.94	.321	.0463
444	2.1	24.9	52.3	114.5	7.10	.331	.0466
462	1.3	27.4	35.6	101.7	7.39	.294	.0398
478	0.7	27.9	20.9	94.1	7.64	.272	.0356
489	0.35	31.5	11.0	89.4	7.82	.258	.0330

B. Rotor and Generator Subsystems

The load power, and total power (shaft power) are given vs. rotational speed in Figure 14 (Runs #4 and #8). Power and torque coefficient plots are given in Figures 15 and 16. Generator efficiency is given in Figures 17 and 18.

CONCLUSIONS AND OBSERVATIONS

A. System Performance

1. Reliability

The Wincharger system proved itself of rugged design and construction. No problems were encountered due to hardware failure; the system is simple and reliable. No vibrations were encountered with the exception of a support-induced mode (observed to occur at about 5 MPH).

In addition to the wind tunnel program, the machine was erected atop one of the engineering buildings on campus for six months, March thru September 1974, and for six months during 1975. No corrosion problems or structural problems were encountered. (The machine did stop due to icing during an ice storm in December 1975). The only failures in the system, which was being used to charge a battery for 12 volt lights, were in the ammeter diodes, which were replaced twice. During the outside experience the surface of the blade did not deteriorate severely. Measurements of the total energy delivered over this period were not taken, and no cumulative system performance testing was done.

2. Observed Output

The manufacturer's specification, charging amperes vs. wind speed, is given in Figure 1; the test results are also given. These results

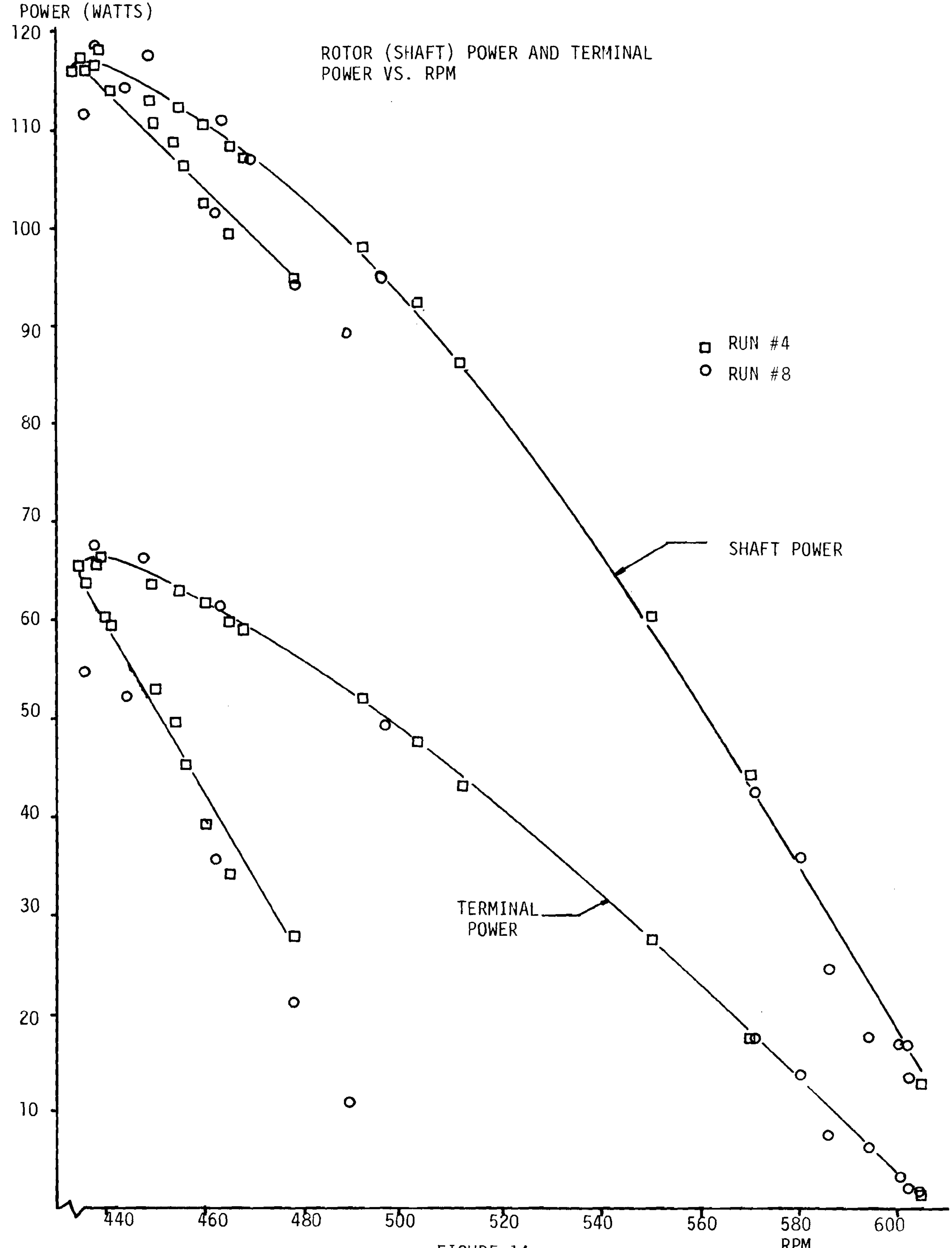
POWER (WATTS)
ROTOR (SHAFT) POWER AND TERMINAL POWER VS. RPM
RUN #4
RUN #8
SHAFT POWER
TERMINAL POWER
RPM
120
110
100
90
80
70
60
50
40
30
20
10
440
460
480
500
520
540
560
580
600

FIGURE 14

ROTOR POWER COEFFICIENT VS. TIP SPEED RATIO
COMPARISON WITH "OPTIMUM" ROTOR

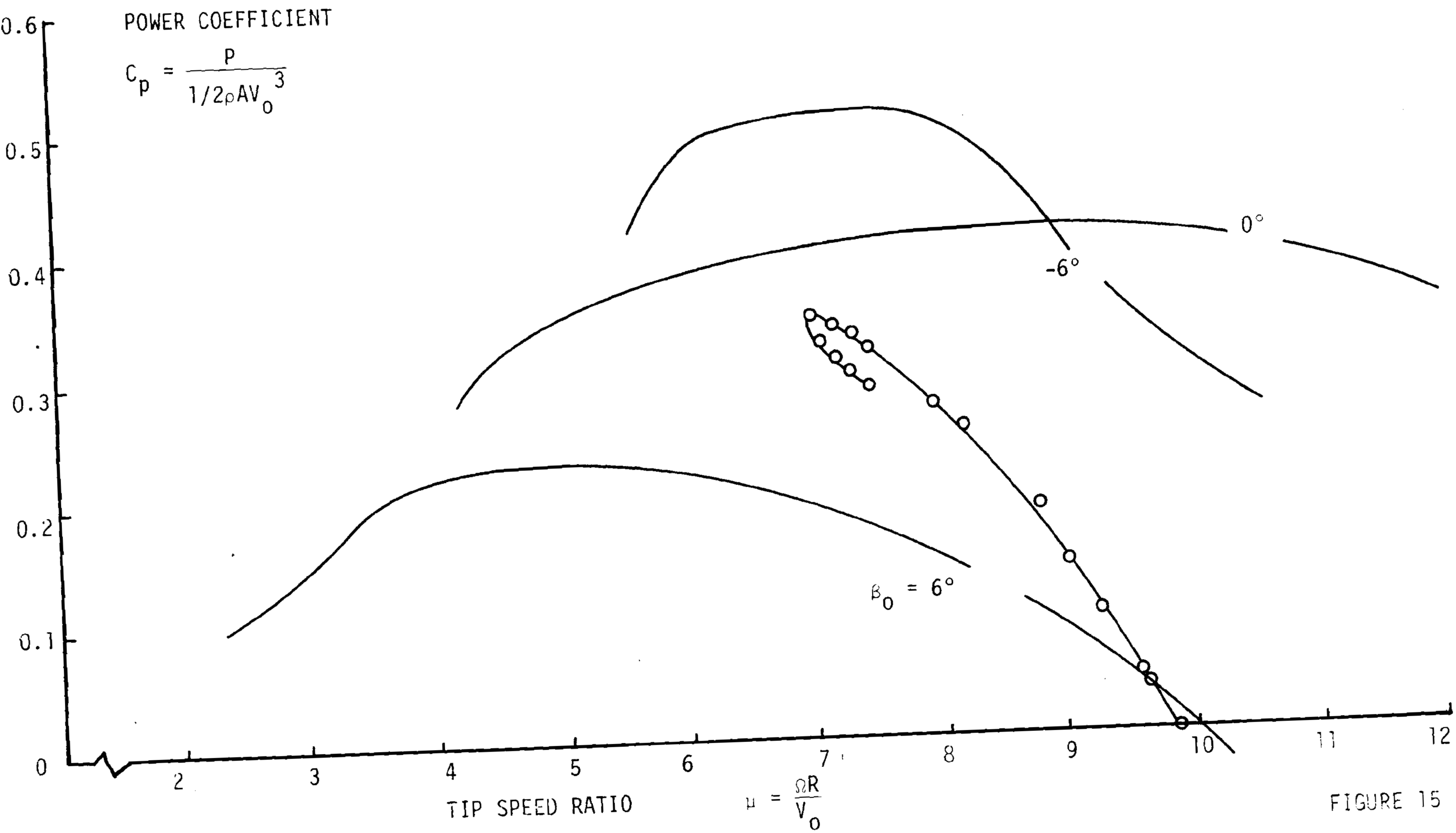

FIGURE 15

TORQUE COEFFICIENT VS. TIP SPEED RATIO
COMPARISON WITH "OPTIMUM" ROTOR

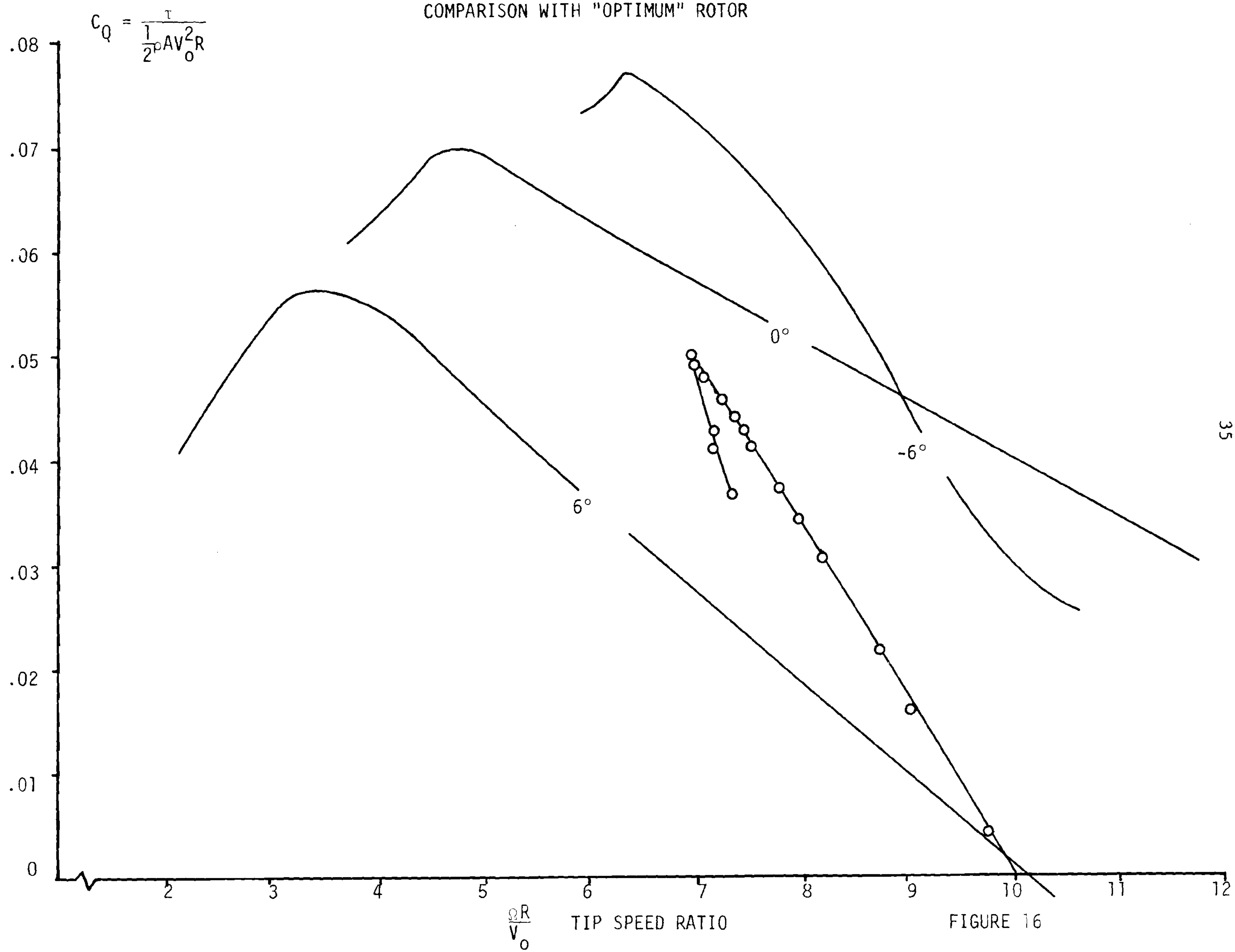

FIGURE 16

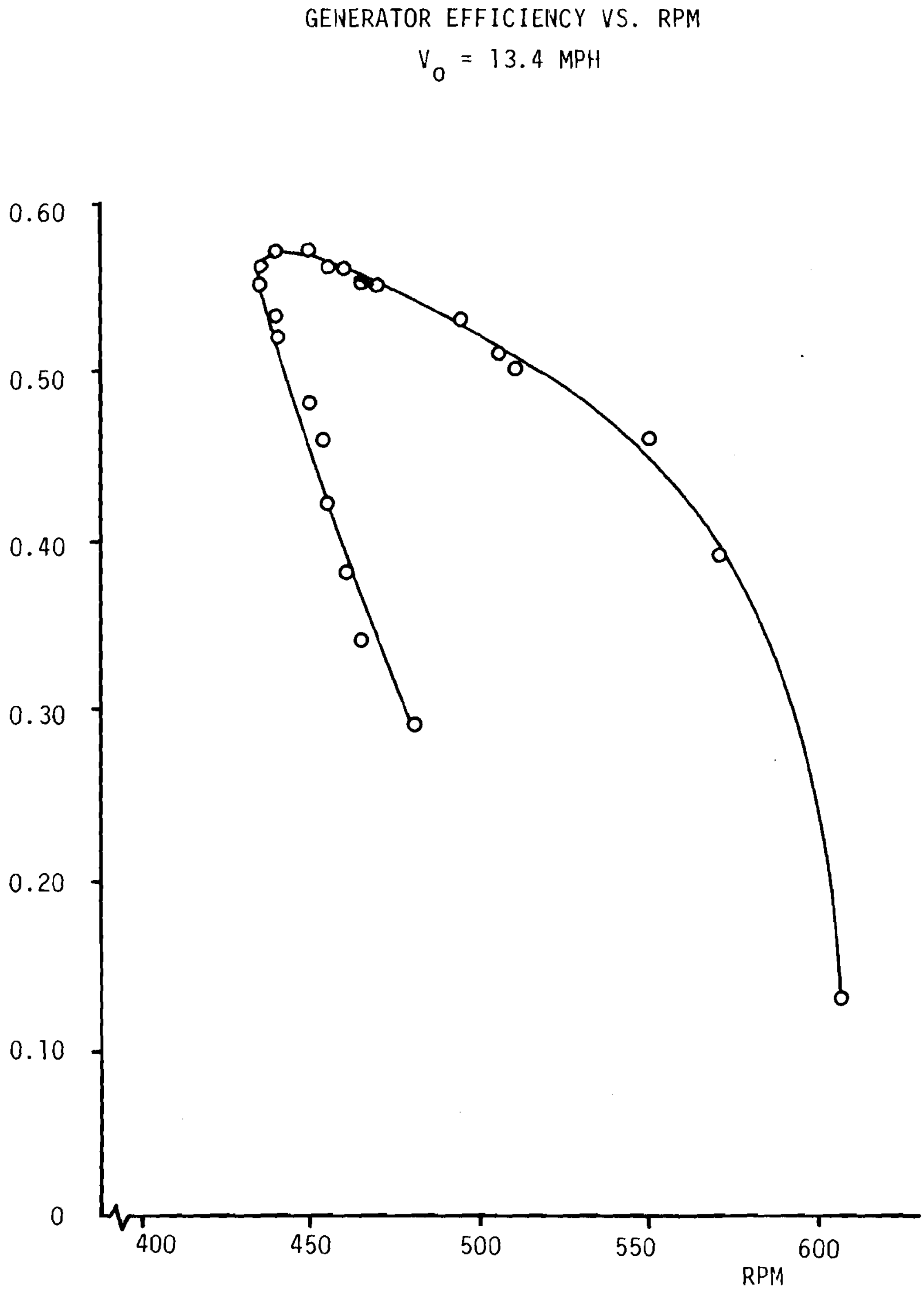
GENERATOR EFFICIENCY VS. RPM
V_0 = 13.4 MPH
0.60
0.50
0.40
0.30
0.20
0.10
0
400
450
500
550
600
RPM

FIGURE 17

GENERATOR EFFICIENCY VS. LOAD RESISTANCE

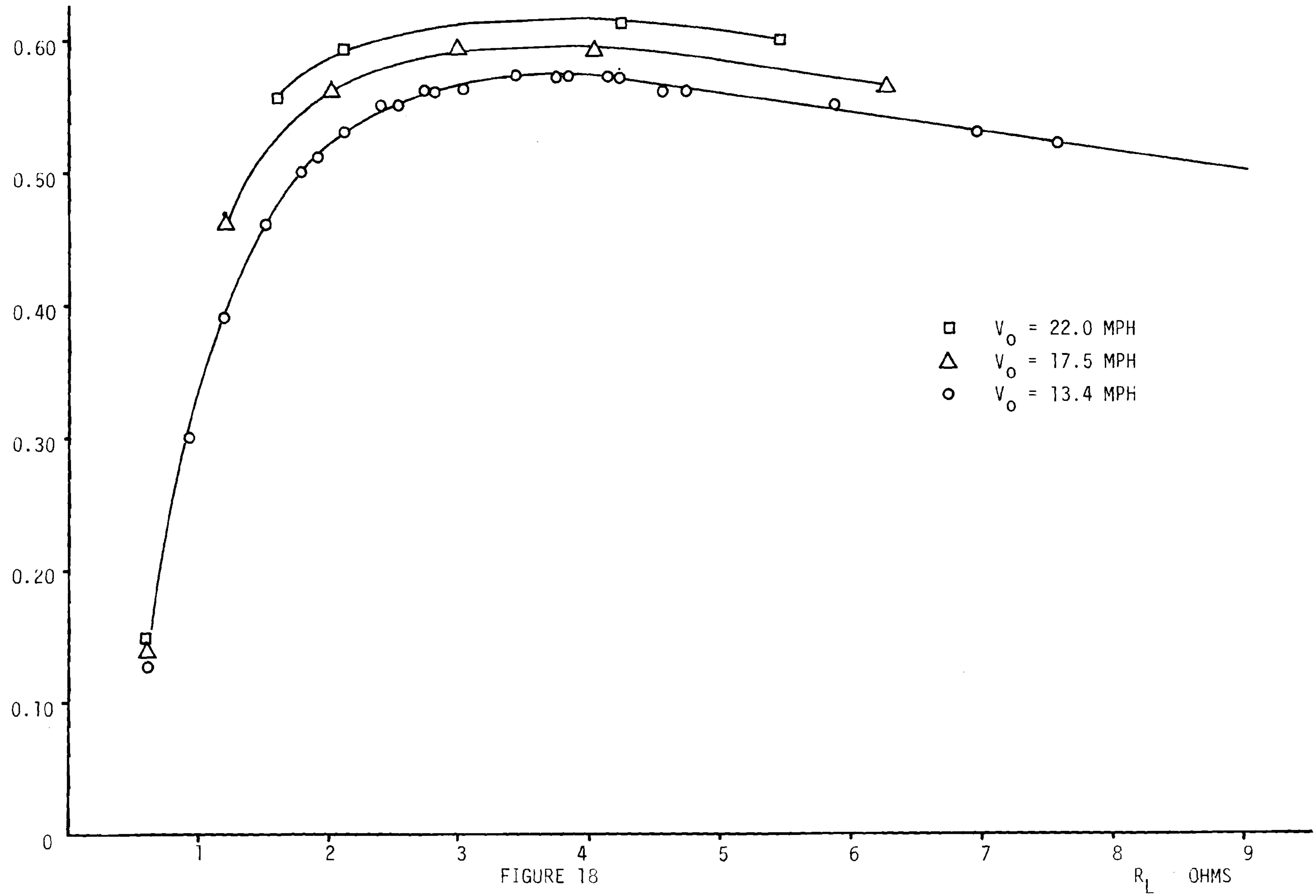

FIGURE 18

are not strictly comparable since the addition of a battery changes the generator load characteristic (the battery voltage acts as a buffer to the shunt field).

The output power vs. rotational speed (Figure 10) illustrates the cubic increase of power with wind speed; the abscissa is RPM, which is proportional to wind speed for a machine with constant tip speed ratio: $\mu = \Omega R/V_0$. For comparison, a curve is shown which is 25% of the available power in the wind ($.25 \times \frac{1}{2}\rho A V_0^3$), for this system. It can be seen that the system delivers less than 25% of the power available, and reaches peak performance at about 700 RPM, at a wind speed of 24 MPH.

3. Control System

The air brake was observed to begin deploying at about 500 RPM; the deployment reaches maximum braking (i.e. maximum area) at about 600 RPM. This behavior is seen in Figure 19, which shows the minimum RPM, or RPM for the highest power, for each wind speed run. The tip speed ratio is close to 7 until 550 RPM is reached; then the curve falls off as drag increases on the air brake, and the tip speed ratio drops.

An ideal control system would keep RPM constant beyond a critical wind speed; this can be done with flyweights (Aerowatt 4.1 kW design) or by pitch variation (NASA-Sandusky wind generator). The simple air brake on this system worked well for wind speeds around 20-30 MPH, but is totally inadequate for higher wind speeds. Since the drag area (of the brake) reaches its maximum at roughly 600 RPM, the drag torque will be proportional to RPM squared; but as wind speed increases, torque

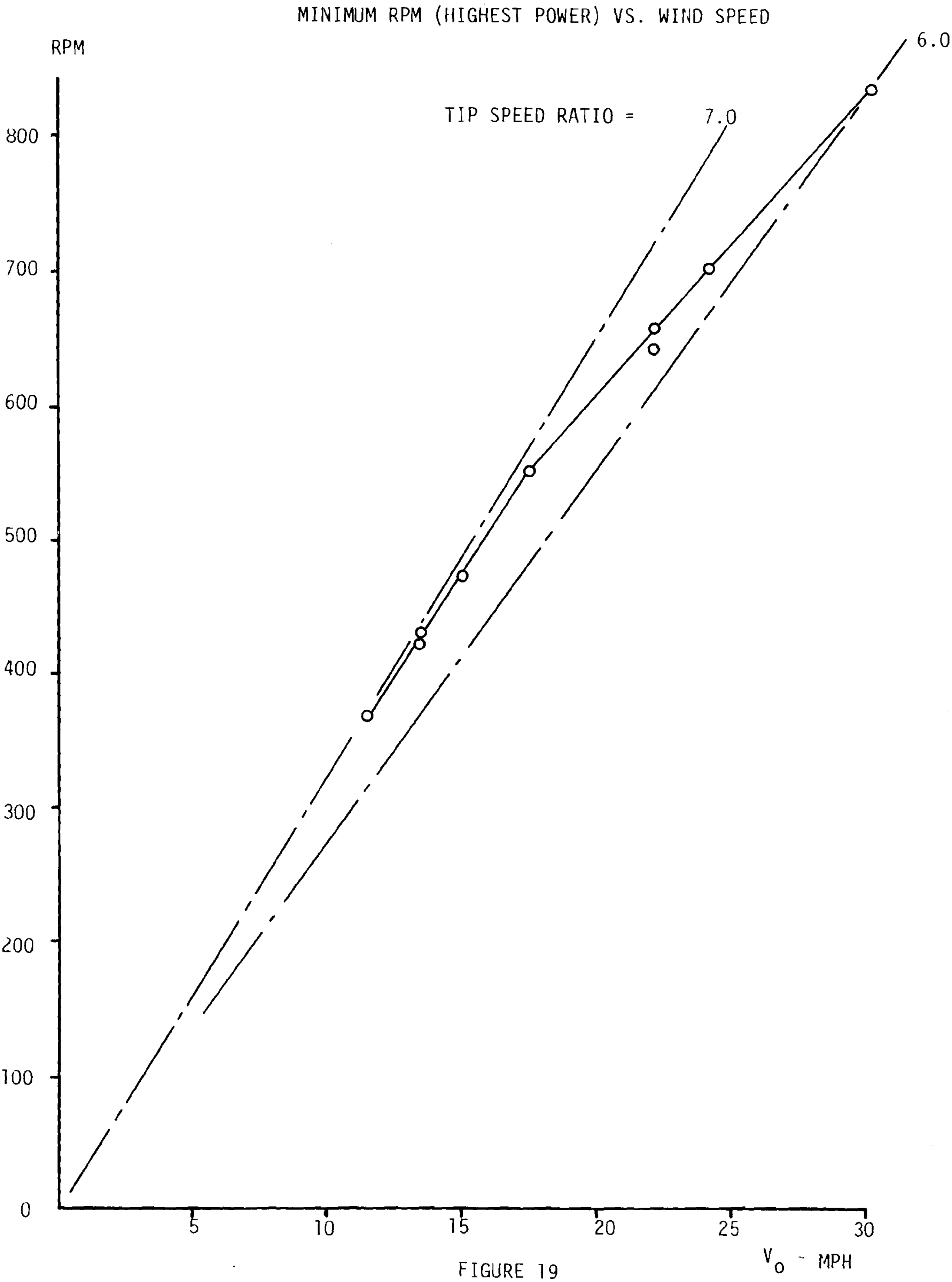
MINIMUM RPM (HIGHEST POWER) VS. WIND SPEED
RPM
TIP SPEED RATIO =
7.0
6.0
800
700
600
500
400
300
200
100
0
5
10
15
20
25
30
V o ~ MPH

FIGURE 19

available increases as V_0^2. If the generator load is constant, the equilibrium governing condition is a constant tip speed ratio, and the curve does not continue to bend over, but is asymptotic to a constant tip speed ratio line (probably $\mu \doteq 6$). In light of this, the manufacturer suggests manually stopping the machine if high winds or storms are expected.

4. Transient Behavior (Changing Load and Start Up)

While data runs were being taken, transient behavior (RPM variation) was allowed to damp out before a data point was read. The time required for the system to reach equilibrium when the load was changed was dependent on the rotational speed. That is, the system would take roughly 5 to 10 revolutions to reach a new equilibrium, regardless of the tunnel speed and absolute RPM. No strict measurements of this were taken due to uncertainties in the wake flow condition. The transient behavior is greatly influenced by the low rotational inertia (low blade weight) of the system. Heavier blades (Appendix 2) took much longer to reach equilibrium.

The start-up behavior of the system was poor. The system was not observed to start by itself at less than 24 MPH tunnel speed, or with loads close to the optimum loading. This is due to the lack of twist in the blade, forcing the total blade into stall at low RPM. This is a characteristic of high speed, low solidity wind generators. At low tunnel speeds, the propeller was given a slight push to start in all cases. It is suspected that in the field usual variations in speed and direction of ambient wind provide the initial rotational motion necessary to start.

B. Propeller Performance

1. Comparison with Optimum Blades

The power coefficient (C_p) and torque coefficient (C_Q) characteristics of the untapered, untwisted Wincharger blade are shown in Figures 15 and 16. Also shown are the predicted characteristics, at fixed pitch settings, of a highly-twisted, highly tapered "optimum" blade (Reference 6). The (set) pitch of the Windcharger blade was not accurately measured, but appeared to be close to flat pitch. The optimum blade was designed for a tip speed ratio of 7, so the results are directly comparable.

The apparent increase in rotor speed after the power peak ("bending back" of the power curve) for the Windcharger is discussed in the next section. In the stable power region (region with negative slope) the untwisted, untapered blade is seen to have a more sensitive characteristic than the optimum blade. Qualitatively, this makes the constant chord blade a "stiffer" dynamic system; that is, the restorative power (and torque) increments due to perturbations in μ will be larger for the untwisted blade than for the optimum blade. This will drive the natural frequency of control instabilities higher for the untapered, untwisted blade. This may be a design consideration, and a trade-off in the control system for the compromised blade. The power peak is also more sensitive to tip speed ratio changes.

Also, the zero slip (zero power) case occurs at a much lower rotational speed for the untwisted, untapered blade (e.g. $\mu \doteq 10$ rather than 14 or 15 for the optimum blade). This is caused by the untwisted blade reaching negative angle of attack, or propeller wake state (see Reference 7), at much larger blade element angles (and much sooner) than the optimum blade. The tip blade elements of the untapered, untwisted blade are already at very low lift coefficients, since circulation is a maximum at the tip, and the corresponding angles of attack are very small (or even negative).

There is an obvious trade-off in cost of manufacture of an optimum blade vs. an untwisted, untapered blade; this trade-off must also involve stability and control considerations as well as compromised performance. This is a very important area for future wind generator rotor testing.

2. Blade Stall

The untwisted, untapered blade is operating most efficiently at its C_p maximum at a tip speed ratio of 7. The blade has stalled root sections; this is true for the entire operating (windmill) range. Moving out on the blade towards the blade tip, the blade element angles decrease rapidly to roughly 8° (1/7) at the tip. The corresponding lift coefficients are low at the (stalled) root, high at the mid-span, and very low at the tip. As the operating point (tip speed ratio) is changed, the lifting condition of the entire blade changes radically. Thus, one would expect a severe stall characteristic for an overloaded condition; that is, if the rotor is loaded beyond the torque available at its optimum tip speed ratio, one would expect a severe stall to occur over the entire blade and the rotor would conceivably come to rest. This (divergent) instability is avoided in the case of the Windcharger, by deliberate undersizing of the generator load. The excitation of the generator is too small to accept a large torque at low RPM (e.g. below

~ 900); thus, as the load resistance is increased, and the field voltage increases, it reaches a "saturation" point beyond which the excitation will decrease. This occurs for this generator before the power peak is reached (see Figure 12). Hence, as R_L is increased, the rotor passes through maximum (system) power and then speeds up as the excitation decreases. This appears as a "bending back" of the power characteristic, even though it is an effect of the other part of the system. If it were possible to test the rotor alone, the characteristic would fall off rapidly as tip speed ratio is decreased below 7. The blade would stall catastrophically as discussed and come to rest. It is suspected that this blade is deliberately oversized (or the generator undersized) to prevent just such a stall; this system is not an optimum power match, for unattended control reasons.

Since this blade could not be loaded deeply into the stalled region by the generator, it was impossible to assess the system performance in the rotor turbulent wake state (Reference 6). The zero slip case (limiting case of propeller state) was observed as discussed by a zero load run, as shown in Figures 15 and 16.

3. Performance Improvements

Glauert's optimum blade design theory for wind generators, neglecting drag (Reference 8), relates optimum tip speed ratio to solidity (total blade area/disc area). Predicted solidity for a propeller with an optimum tip speed ratio of 7, is 8%; for a tip speed ratio of unity (e.g. American fan mill) the optimum solidity is 98%. The untwisted, untapered Wincharger blade has a solidity ($= BC/\pi R$) of 6.2%. The Glauert theory (Ref. 8) would predict an optimum tip speed ratio of 9 for this solidity, provided the blade was of optimum twist and taper.

Since the blade is highly compromised (untwisted and untapered), and the root sections are thus stalled, one would expect the optimum tip speed ratio to occur when the spanwise circulation distribution was most favorable. This distribution can obviously be changed by adjusting pitch, and as the curves of optimum fixed pitch machines show (Figures 15 and 16), optimum tip speed ratios as well as maximum power coefficients can be adjusted.

Two-bladed model propellers, all constant chord, but with high twist according to the Glauert theory, were constructed during a windpower workshop course. The blades were of different airfoils and all had roughly 25° of twist, mostly in the inner half of the blade. Chords were chosen to give solidity of 6.2% (c = 3.5") to compare with the Wincharger blade. The blades had steel rods for a main spar at the quarterchord, with paper honeycomb cores and fiberglas laminate skin. This blade construction technique was first proposed by Hans Meyer of Windworks (Reference 9). Due to the blade inaccuracies and surface roughness, the test results are not considered as accurate and useful as the Wincharger results of this report. Nevertheless, a certain trend is shown. Figure 20 gives the RPM vs. wind speed (tip speed ratio) curve, and Figure 21 gives the power characteristic for the blades compared with the untwisted, untapered blade. As can be seen in Figure 21, the model blades all showed higher performance than the untwisted blade. Part of this improvement is attributable to the exclusion of the friction brake drum and its wake blockage. Estimates of this effect were not made; however, most of the improvement in power coefficient, especially at low speeds where the friction drag is

RPM VS. WIND SPEED (MODEL BLADES)

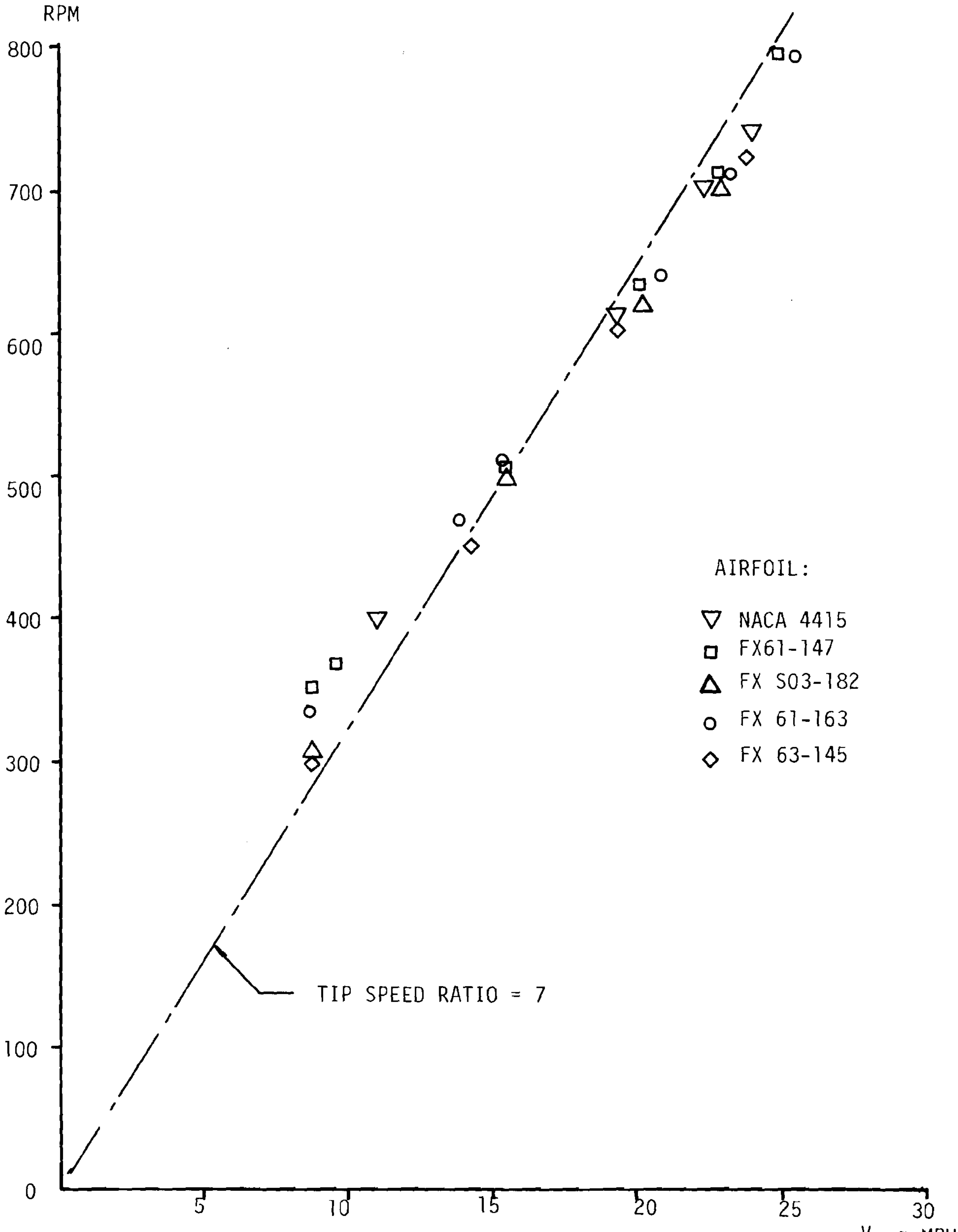

FIGURE 20

POWER VS. WIND SPEED (MODEL BLADES)

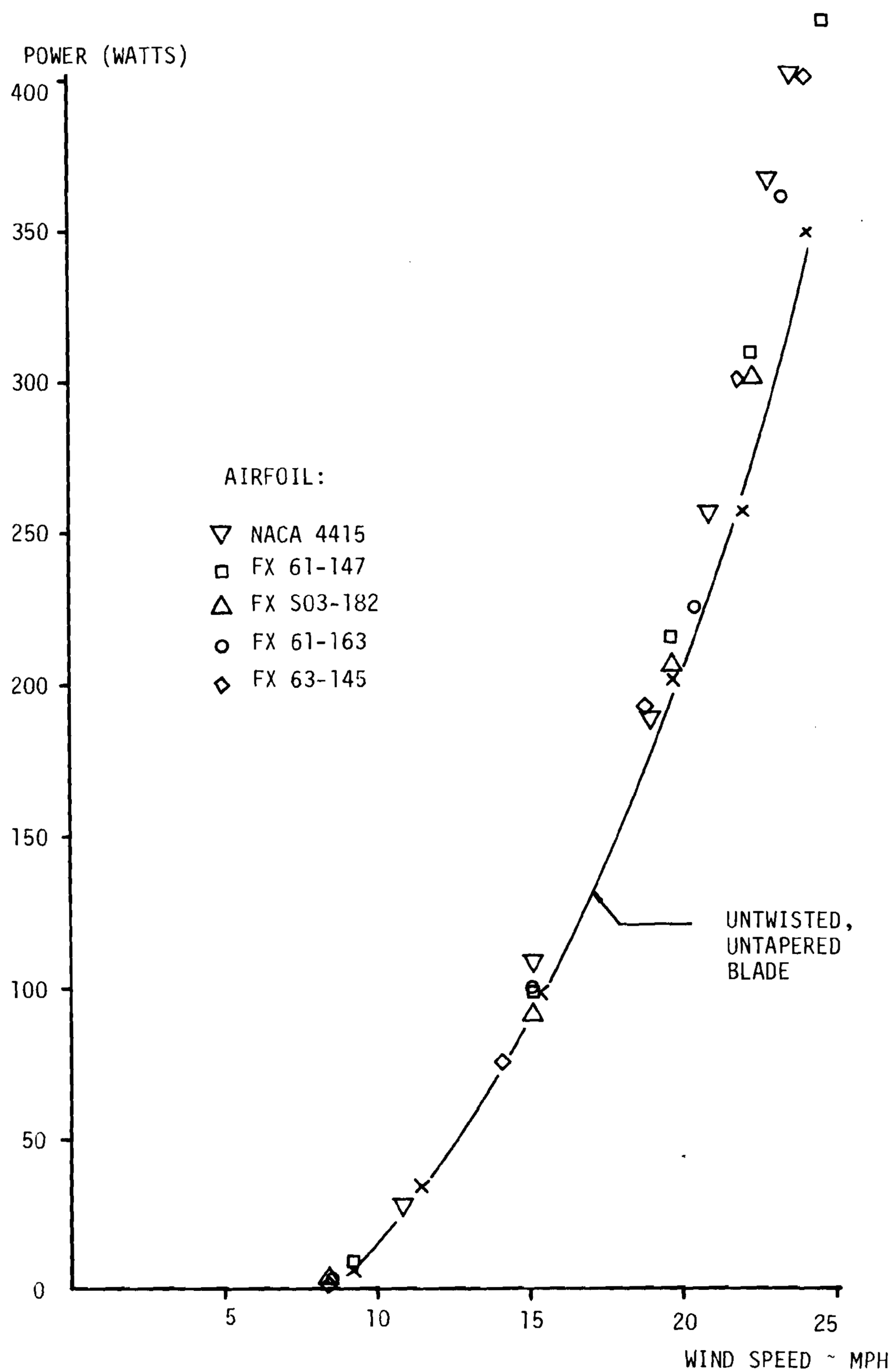

FIGURE 21

less predominant, is due to the favorable twist distributions. Figure 20 shows the resultant tip speed ratios all to be near the design goal of 7.0. In Appendix 2 is given the tunnel test data for these model blades.

REFERENCES

1. Instructions for Assembly of Model 1222 Wind-Driven Generator Plant; Winco, Division of Dyna Technology, Inc., Sioux City, Iowa.

2. Poole, D.B., and Cromack, D.E., "Defining the Flow Field of an Open-Jet Wind Tunnel," Themis Report No. THEMIS-UM-70-3, University of Massachusetts, June 1970.

3. "Investigation of the Feasibility of Using Windpower for Space Heating in Colder Climates," Fourth Quarterly Progress Report, NSF/RANN/AER-75-00603/PR/76/1, March 1976.

4. Personal Communication with Dr. Doug Taff, Garden Way Associates, Charlotte, Vermont, September 1974.

5. Prandtl, L., and Tietjens, O.G., Applied Hydro and Aeromechanics, Dover Publication, Inc., New York, 1934.

6. Stoddard, F.S., "An Approach to Preliminary Systems Optimization of the New England Wind Furnace," Appendix V, Fourth Quarterly Progress Report, "Investigation of the Feasibility of Using Windpower for Space Heating in Colder Climates," Report NSF/RANN/AER-75-00603/PR/76/1, March 1976.

7. Stoddard, F.S., "Discussion of Momentum Theory for Windmills," Appendix IV, Fourth Quarterly Progress Report, "Investigation of the Feasibility of Using Windpower for Space Heating in Colder Climates," Report NSF/RANN/AER-75-00603/PR/76/1, March 1976.

8. Glauert, H., "Windmills and Fans," Aerodynamic Theory, Vol. IV, Dover Publications, 1963.

9. Meyer, Hans, "Twelve Footer Plans: Blade Construction," Windworks, Mukwonago, Wisconsin, 1973.

APPENDIX 1

TUNNEL TEST DATA

RUN #1 No Load (R = 0) 1520:time

(± .002)

Manometer height (in.)	V MPH	RPM equil.
b) .055	9.5	b) 400
a) .050	9.2	a) 130
.075	11.1	480
.110	13.5	595
.150	15.5	695
.168	16.6	710
.175	17.0	740
.200	18.2	800
.215	18.9	800
.240	20.0	820
.285	21.6	860
.320	22.9	900
.355	24.0	940
.375	24.8	960
.400	25.5	1000
.440	26.7	1025
.460	27.3	1040
.475	27.8	1050
.500	28.5	1070

RUN #3

$h = .08$ in.
$V = 11.4$ MPH

$$\text{torque} = \frac{\text{watts}}{\text{RPM}}(7.04037)$$

R Ω	I amp	E_t v	P watts	RPM	Torque (ft-lb)
25.625	.8	20.5	16.4	390	.296
10.42	1.65	17.2	28.38	375	.533
6.5	2.4	15.6	37.44	370	.712
5.92	2.4	14.2	34.08	372	.65
5.15	2.6	13.4	34.84	374	.66
4.7	2.7	12.7	34.29	375	.64
4.39	2.8	12.3	34.44	377	.64
4.07	2.9	11.8	34.22	382	.63
2.58	3.3	8.5	28.05	415	.48
2.246	3.25	7.3	23.73	430	.39
2.06	3.2	6.6	21.12	439	.34
1.93	2.9	5.6	16.24	456	.25
1.71	2.8	4.8	13.44	465	.20
1.417	2.4	3.4	8.16	480	.12
1.238	2.1	2.6	5.46	485	.08
.769	1.3	1.0	1.3	498	.02
∞	0	24.5	-	412	0
14.62	1.3	19.0	24.6	380	

RUN #4

h = 0.11 in
v = 13.4 MPH

R Ω	I amp	E_t v	P watts	RPM	Torque (ft-lb)
29.684	.95	28.2	27.79	478	.41
21.76	1.25	27.2	34	465	.51
17.47	1.5	26.2	39.3	460	.60
13.94	1.8	25.1	45.18	456	.70
11.805	2.05	24.2	49.61	454	.77
10.40	2.25	23.4	52.65	450	.82
10.36	2.25	23.3	52.43	450	.82
7.57	2.8	21.2	59.36	441	.95
6.95	2.95	20.5	60.48	440	.97
5.85	3.3	19.3	63.69	436	1.03
5.67	3.3	18.7	61.71	437	.99
4.81	3.7	17.8	65.86	435	1.07
4.64	3.75	17.4	65.25	434	1.06
4.33	3.9	16.9	65.91	438	1.06
4.15	4.0	16.6	66.4	439	1.06
3.95	4.1	16.2	66.42	438	1.07
3.76	4.2	15.8	66.36	439	1.06
3.53	4.25	15.0	63.75	449	1.00
3.11	4.5	14.0	63.0	455	.97
2.98	4.6	13.7	63.02	455	.97
2.787	4.7	13.1	61.57	460	.94
2.653	4.75	12.6	59.85	465	.91
2.563	4.8	12.3	59.04	468	.89
2.163	4.9	10.6	51.94	492	.74
2.02	4.85	9.8	47.53	503	.66
1.875	4.8	9.0	43.2	512	.59
1.634	4.1	6.7	27.47	550	.35
1.333	3.6	4.8	17.28	570	.21
.71	1.55	1.1	1.705	604	.02
∞	0	30		497	

RUN #5 $h = 0.185$ in
$v = 17.5$ MPH

R Ω	I amp	E_t v	P ω	RPM	Torque
10.45	3.35	35.0	117.25	578	1.43
7.05	4.4	31.0	136.4	556	1.73
6.93	4.4	30.5	134.2	?	--
6.34	4.65	29.5	137.18	555	1.74
5.878	4.9	28.8	141.12	550	1.81
5.49	5.1	28.0	142.8	550	1.83
4.29	5.85	25.1	146.84	550	1.88
4.12	6.0	24.7	148.2	550	1.90
3.93	6.1	24.0	146.4	550	1.87
3.90	6.15	24.0	147.6	550	1.89
3.90	6.15	24	147.6	550	1.89
3.45	6.5	22.4	145.6	556	1.84
3.28	6.65	21.8	144.97	558	1.83
3.04	6.9	21	144.9	561	1.82
2.72	7.2	19.6	141.12	574	1.73
2.22	7.4	16.4	121.36	609	1.40
2.07	7.5	15.5	116.25	621	1.32
1.97	7.6	15.0	114.0	619	1.30
1.72	7.15	12.3	87.95	656	.94
1.33	6.0	8.0	48.0	710	.48
1.08	2.85	3.1	8.835	755	.08
0.664	1.9	1.3	2.47	765	.02

RUN #7

h = 0.295 in
v = 22 MPH

R Ω	I amp	E_t v	P watts	RPM	Torque
5.5	6.75	37.2	251.1	655	2.66
4.35	7.7	33.5	257.95	659	2.76
3.95	8.1	32.0	259.2	655	2.78
3.95	8.1	32.0	259.2	664	2.75
3.926	8.1	31.8	257.58	669	2.71
3.37	8.75	29.5	258.13	659	2.76
3.186	8.85	28.2	249.57	676	2.60
3.056	9.6	27.5	247.5	683	2.56
2.757	9.25	25.5	235.88	695	2.39
2.172	9.3	20.2	187.86	730	1.81
2.087	9.2	19.2	176.64	745	1.67
1.99	9.3	18.5	172.05	755	1.60
1.744	8.6	15.0	129.0	765	1.19
1.35	6.6	8.9	58.74	820	.50
1.10	3.9	4.3	16.77	835	.14
.683	1.8	1.23	2.21	848	.02

RUN #8

h = 0.11 in.
v = 13.4 MPH

R	I	E	P	RPM	Torque
.81	1.5	1.21	1.82	604	.02
.91	1.53	1.39	2.13	602	.02
1.06	1.8	1.90	3.42	602	.04
1.07	1.8	1.92	3.46	600	.04
1.08	1.85	2.0	3.70	594	.043
1.18	2.05	2.42	4.96	598	.06
1.34	2.35	3.15	7.40	586	.09
1.52	3.0	4.55	13.65	580	.17
1.61	3.3	5.3	17.49	571	.22
1.88	5.1	9.6	48.96	496	.69
2.43	4.9	11.9	58.31	468	.88
2.51	4.95	12.4	61.38	463	.48
3.0	4.7	14.1	66.27	448	1.04
3.50	4.4	15.4	67.76	438	1.09
5.82	3.35	19.5	65.33	422	1.09
9.5	2.4	22.8	54.72	434	.89
11.86	2.1	24.9	52.29	444	.83
21.08	1.3	27.4	35.62	462	.54
42.71	0.7	29.9	20.93	478	.31
90.0	0.35	31.5	11.03	489	.16

RUN #9

h = .295 in.
v = 22.0 MPH

R	I	E	P	RPM
.73	2.2	1.6	3.52	855
.87	2.75	2.4	6.6	855
.93	2.9	2.7	7.83	860
1.03	3.7	3.8	14.06	850
1.12	4.45	5.0	22.25	840
1.12	5.25	5.9	30.98	830
1.13	5.4	6.1	32.94	830
1.24	7.0	8.7	60.9	810
1.36	8.95	12.2	109.19	780
1.44	9.0	13.0	117.0	775
1.60	10.0	16.0	160.0	745
1.74	10.25	17.8	182.5	725
1.83	10.35	18.9	195.6	715
1.96	10.5	20.6	216.3	700
2.18	10.4	22.7	236.1	680
2.38	10.25	24.4	250.1	666
2.69	9.85	26.5	261.0	656
3.06	9.35	28.6	267.4	645
3.33	9.0	30.0	270.0	640
4.28	8.0	34.2	273.6	640
5.47	6.95	38.0	264.1	650

RUN #10 h = .355 in.
v = 24 MPH

R	I	E	P	RPM	Torque
.74	2.15	1.59	3.42	925	.026
.81	2.35	1.9	4.47	925	.034
.89	2.8	2.5	7	730	.05
.94	3.1	2.9	9	920	.07
1.01	3.75	3.8	14.25	920	.11
1.05	4.25	4.55	19.79	920	.15
1.11	5.5	6.1	33.55	905	.26
1.11	6.15	6.85	42.13	905	.33
1.18	7.7	9.1	70.07	880	.56
1.29	9.05	11.7	105.89	860	.87
1.92	10.1	14.3	144.4	835	1.22
1.55	11.0	17.0	187.0	810	1.63
1.72	11.65	20.0	233.0	790	2.08
1.86	11.95	22.2	365.3	775	2.41
2.13	11.85	25.2	298.6	750	2.80
2.38	11.5	27.4	315.1	730	3.04
2.46	11.45	28.2	322.9	720	3.16
2.99	10.65	31.8	338.7	705	3.38
3.47	10.0	34.7	347.0	700	3.49
4.18	9.1	38.0	345.8	700	3.48
5.17	8.05	41.6	334.9	710	3.32
6.84	6.8	46.5	316.2	735	3.03

RUN #11

h = 0.14 in.
v = 15 MPH

R	I	E	P	RPM	Torque
.75	1.6	1.2	1.92	674	.02
.85	1.65	1.41	2.33	673	.024
.97	1.85	1.8	3.33	669	.035
1.20	2.3	2.75	6.33	665	.067
1.31	2.75	3.6	9.9	660	.11
1.40	3.4	4.75	16.15	649	.18
1.48	4.45	6.6	29.37	625	.33
1.61	4.65	7.5	34.88	620	.40
1.68	5.3	8.9	47.2	599	.55
1.81	5.65	10.2	57.6	580	.70
1.97	5.9	11.6	68.4	554	.87
2.13	6.0	12.8	76.8	542	1.00
2.41	5.9	14.2	83.8	524	1.13
2.51	5.9	14.8	87.3	520	1.18
3.01	5.65	17.0	96.05	496	1.36
4.16	4.9	20.4	99.96	479	1.47
5.23	4.15	21.7	90.1	475	1.34
5.26	4.3	22.6	97.2	472	1.45
6.90	3.65	25.2	91.98	481	1.35
10.21	2.8	28.6	80.1	500	1.13
21.42	1.55	33.2	51.46	526	.69
42.0	.85	35.7	30.35	550	.39
84.44	.45	38.0	17.10	558	.22

RUN #12

h = .55 in.
v = 30 MPH

R	I	E	P	RPM	Torque
.70	2.65	1.85	4.9	1120	.031
.77	3.1	2.4	7.4	1110	.05
.89	3.95	3.5	13.8	1110	.09
.99	7.55	7.5	56.6	1090	.37
1.08	9.25	10.0	92.5	1070	.61
1.20	11.6	13.9	161.2	1050	1.08
1.34	13.4	18.0	241.2	1015	1.67
1.41	14.5	20.5	297.3	995	2.10
1.51	14.9	22.5	335.3	970	2.43
1.56	15.1	23.6	356.4	960	2.61
2.61	14.6	38.1	556.3	855	4.58
2.94	13.9	40.8	567.1	840	4.75
3.45	12.8	44.2	565.8	835	4.77
4.07	11.8	48.0	566.4	850	4.69
5.0	10.4	52.0	540.8	865	4.40

RUN #13

Velocity Survey
Req ≃ 2.57Ω

h in.	V MPH	I amp	E_t v	P watt	Req Ω	RPM
.045	8.7	1.2	3.35	4.02	2.79	363
.070	10.6	2.85	7.5	21.38	2.63	420
.085	11.7	3.35	8.4	28.14	2.51	446
.085	11.7	3.34	8.7	30.02	2.52	440
.095	12.3	4.0	10.1	40.4	2.53	464
.100	12.7	4.3	11.0	47.3	2.56	475
.12	13.9	5.3	13.6	72.08	2.57	500
.14	15.0	6.1	15.5	94.55	2.54	526
.15	15.5	6.5	16.3	105.95	2.51	536
.18	17.2	7.3	19.0	138.7	2.60	569
.215	18.7	8.35	21.3	177.86	2.55	606
.235	19.7	8.9	23.6	210.04	2.65	636
.250	20.2	9.4	24.0	225.6	2.55	653
.270	21.1	9.8	25.2	246.96	2.57	682
.295	22.0	10.3	26.5	272.95	2.57	700
.315	22.7	10.85	27.8	301.63	2.56	715
.335	23.4	11.35	28.7	325.75	2.53	737
.370	24.5	11.75	30.0	352.5	2.55	762
.395	25.3	12.0	30.9	370.8	2.57	786
.415	26.0	12.6	31.9	401.94	2.53	800
.435	26.7	12.8	32.7	418.56	2.55	815
.455	27.2	13.0	33.5	435.5	2.58	835
.475	27.8	13.15	34.0	447.1	2.59	845
.490	28.2	13.45	34.3	461.39	2.55	865
.515	28.8	13.8	35.0	483.0	2.54	885
.535	29.4	13.9	35.7	496.23	2.57	900
.550	29.8	14.2	35.8	508.36	2.52	915
.560	30.2	14.2	36.2	514.04	2.55	930
.595	31.1	14.65	37.3	546.45	2.55	955
.605	31.3	14.7	37.4	549.79	2.54	970
.625	31.8	14.9	37.7	561.73	2.53	990
.635	32.3	15.0	38.0	570.0	2.53	1005

RUN #14

Velocity Survey
Req ≃ 3.95Ω

h in.	V MPH	I amp	E v	P watt	Req Ω	RPM
.055	9.5	1.75	7.0	12.25	4.0	353
.075	11.1	2.55	10.0	25.50	3.9	410
.10	12.8	3.35	13.6	45.56	4.06	447
.125	14.2	4.5	17.8	80.10	3.96	484
.160	16.2	5.4	21.5	116.10	3.98	530
.180	17.2	6.0	23.8	142.80	3.97	559
.215	18.8	6.75	26.4	178.20	3.91	600
.240	20.0	7.35	28.9	212.41	3.93	634
.270	21.2	7.9	31.2	296.48	3.95	666
.310	22.5	8.8	34.6	304.48	3.93	710
.345	23.7	9.3	36.5	339.45	3.92	738
.370	24.5	9.5	37.6	357.2	3.96	755
.400	25.5	10.0	39.3	393.0	3.93	780
.420	26.5	10.25	40.5	415.13	3.95	810
.460	27.4	10.6	41.9	444.14	3.95	835
.480	27.9	10.85	43.0	466.55	3.96	855
.495	28.3	11.15	44.0	490.60	3.95	870
.520	29.0	11.3	44.7	505.11	3.96	885
.555	30.0	11.65	46.0	535.9	3.95	910
.560	30.3	12.0	46.9	562.8	3.91	925
.595	31.2	12.2	47.7	581.94	3.91	945
.610	31.6	12.35	48.3	596.51	3.91	960
.635	32.3	12.6	49.7	626.2	3.94	970

RUN #15 Velocity Survey
Req ≅ 4.70Ω

h in.	V MPH	I	E	P	Req	RPM
.05	9.2	1.1	5.5	6.05	5.0	362
.06	10.0	1.65	8.2	13.53	4.97	368
.08	11.5	2.45	11.4	27.93	4.65	411
.11	13.4	3.6	17.3	62.28	4.81	460
.155	15.7	4.8	22.7	108.96	4.73	524
.200	18.2	5.85	27.5	160.87	4.70	582
.245	20.2	6.8	32.2	218.96	4.73	637
.300	22.3	7.7	36.0	277.20	4.68	688
.350	23.8	8.5	39.5	335.75	4.65	735
.415	26.0	9.3	43.4	403.62	4.67	790
.460	27.3	9.9	45.5	450.45	4.60	830
.500	28.5	10.2	47.5	484.5	4.66	860
.545	29.7	10.8	49.8	537.8	4.61	890

RUN #16

Velocity Survey
Req ≈ 5.65Ω

h	V	I	E	P	Req	RPM
.05	9.2	1.15	7.3	8.39	6.35	362
.07	10.8	1.95	12.0	23.4	6.15	393
.105	13.0	3.05	18.5	56.42	6.07	445
.155	16.0	4.3	24.9	107.07	5.79	525
.195	18.0	5.1	29.5	150.45	5.78	575
.230	19.5	6.0	33.7	202.2	5.62	628
.280	21.4	6.6	37.6	248.16	5.70	677
.350	23.8	7.5	42.5	318.75	5.67	750
.410	25.7	8.3	46.8	388.44	5.64	795
.440	26.7	8.65	47.2	408.28	5.46	825
.475	27.7	9.0	50.0	450.0	5.56	850
.505	28.6	9.2	52.0	488.4	5.65	870
.595	29.6	9.6	54	518.4	5.63	900
.590	31.0	10.2	57	581.4	5.59	950

RUN #17

Velocity Survey
Req ≈ .73 (lowest value)

h	V	I	E	P	Req	RPM
.04	8.3	0.8	.7	.56	.88	335
.07	10.7	1.1	.9	.99	.82	477
.11	13.3	1.35	1.1	1.48	.81	595
.16	16.2	1.55	1.2	1.86	.77	710
.205	18.3	1.70	1.3	2.21	.76	760
.250	20.3	1.85	1.35	2.50	.73	810
.30	22.2	2.0	1.45	2.90	.73	850
.35	23.8	2.05	1.5	3.07	.73	900
.405	25.7	2.10	1.55	3.25	.74	960
.440	26.7	2.15	1.6	3.44	.75	1005
.490	28.2	2.20	1.6	3.52	.73	1050
.525	29.2	2.2	1.6	3.52	.73	1075
.560	30.2	2.2	1.6	3.52	.73	1110
.590	31.0	2.2	1.6	3.52	.73	1150
.630	32.0	2.2	1.6	3.52	.73	1190
.640	32.3	2.2	1.6	3.52	.73	1200

RUN #18

Velocity Survey
Req ≐ 1.69Ω

h	V	I	E	P	Req	RPM
.045	9.0	.95	1.9	1.81	2.0	364
.065	10.5	1.5	2.65	3.98	1.77	445
.095	12.3	2.8	4.75	13.3	1.70	527
.125	14.3	5.0	8.3	41.5	1.66	577
.155	15.7	6.25	11.0	68.75	1.76	616
.190	17.7	7.4	12.8	94.72	1.73	669
.23	19.5	8.55	14.9	127.4	1.74	715
.285	21.6	10.0	17.0	170.0	1.70	760
.34	23.6	11.0	18.6	204.6	1.69	800
.38	24.9	11.8	20.0	236.0	1.69	835
.425	26.2	12.6	21.0	264.6	1.67	870
.465	27.4	13.2	22.0	290.4	1.67	890
.49	28.2	13.35	22.2	296.4	1.66	905
.50	28.5	13.1	22.6	296.06	1.73	915
.51	28.7	13.9	23.0	319.7	1.65	920
.515	28.8	13.9	23.3	323.9	1.68	940
.530	29.3	14.4	24.0	345.6	1.67	970
.565	30.3	14.95	25.0	373.8	1.67	990
.585	30.8	>15	25.5			

RUN #19 h = .048 in.
v = 9.0 MPH

R	I	E	P	RPM
.93	1.0	.93	.93	--
.90	1.0	.90	.90	384
1.1	1.0	1.1	1.1	380
1.3	1.0	1.3	1.3	378
1.45	1.0	1.45	1.45	381
1.6	1.0	1.6	1.6	381
1.8	1.0	1.8	1.8	379
1.95	1.0	1.95	1.95	377
2.1	1.0	2.1	2.1	375
2.55	1.0	2.55	2.55	377
2.9	1.0	2.9	2.9	371
3.0	1.1	3.3	3.63	370
3.36	1.1	3.7	4.07	368
3.63	1.2	4.35	5.22	364
3.64	1.1	4.0	4.4	370
4.24	1.25	5.3	6.63	356
4.72	1.25	5.9	7.38	353
5.0	1.25	6.25	7.81	350
5.31	1.3	6.9	8.97	344
6.16	1.25	7.7	9.63	336
6.83	1.2	8.2	9.84	334
8.18	1.1	9.0	9.90	330
10.0	1.0	10.0	10.0	326
13.76	.85	11.7	9.95	320
19.54	.65	12.7	8.26	322
40.57	.35	14.2	4.97	322
∞	0	16.0	0	329

A P P E N D I X 2

Model Blades:
Tunnel Test Data

BLADE PROFILE	V_o (MPH)	RPM	R_L	E_t	I_L	P(watts)
NACA 4415	10.7	395	2.6	7.4	2.8	20.72
	15.0	500	"	16.2	6.4	103.68
	18.7	595	"	21.6	8.4	181.4
	20.1	665	"	25.0	9.9	247.5
	22.8	720	"	30.0	11.7	351.0
	23.5	760	"	31.5	12.3	387.45
	24.8	800	"	34.0	13.4	455.6
	10.7	360	4.2	10.8	2.6	28.08
	15.0	490	"	21.2	5.1	108.12
	18.7	575	"	28.0	6.75	189.0
	20.7	645	"	32.5	7.9	256.75
	22.8	715	"	39.0	9.4	366.6
	23.5	740	"	41.0	9.8	401.8
	24.8	800	"	44.5	10.7	476.15
Fx 63-145	8.3	290	2.6	1.4	0.6	0.84
	13.9	440	"	13.5	5.4	72.9
	18.7	590	"	21.5	8.5	182.75
	21.8	690	"	27.0	10.65	287.6
	24.2	780	"	32.0	12.4	396.8
	8.3	290	4.2	1.95	.55	1.07
	13.9	435	"	17.5	4.25	74.38
	18.7	575	"	28.2	6.8	191.76
	21.8	680	"	35.5	8.45	300.0
	24.2	760	"	42.0	10.0	400
Fx 61-147	9.2	360	2.6	2.8	1.2	3.36
	15.0	495	"	15.3	6.1	73.3
	19.5	620	"	23.2	9.0	208.8
	22.2	700	"	27.5	10.7	294.25
	24.5	780	"	32.2	12.6	405.7
	9.2	335	4.2	5.9	1.5	8.85
	15.0	470	"	20.0	4.9	98.0
	19.5	600	"	30.0	7.2	216.0
	22.2	680	"	35.8	8.5	308.3
	24.5	760	"	41.8	10.0	418.0

BLADE PROFILE	V_o(MPH)	RPM	R_L	E_t	I_L	P(Watts)
Fx 6 1-163	8.2	325	2.6	2.27	1.0	2.27
	15.0	500	"	15.7	6.1	95.8
	20.3	630	"	23.5	9.3	218.6
	23.2	730	"	30.0	11.7	351.0
	8.2	320	4.2	3.3	9	2.97
	15.0	475	"	20.0	5.0	100.0
	20.3	610	"	30.5	7.4	225.7
	23.2	710	"	39.0	9.3	362.7
Fx S03-182	8.3	300	2.6	1.6	0.7	1.12
	15.0	490	"	14.5	5.85	54.83
	19.5	605	"	22.2	8.75	194.85
	22.2	690	"	27.0	10.6	286.2
	25.8	815	"	34.2	13.45	460.0
	8.3	300	4.2	2.15	.65	1.4
	15.0	460	"	19.5	4.7	91.7
	19.5	590	"	29.2	7.05	205.9
	22.2	680	"	35.2	8.5	299.2
	25.8	800	"	44.5	10.75	478.4